Supporting Information

for

Remote control of the reversible assembly/disassembly of supramolecular aggregates

Nikita Mittal, Indrajit Paul, Susnata Pramanik, Michael Schmittel*

Center of Micro and Nanochemistry and Engineering, Organische Chemie I, Universität Siegen, Adolf-Reichwein Str. 2, 57068 Siegen, Germany

E-mail: schmittel@chemie.uni-siegen.de

Table of Contents

Abbreviations:

DCM : dichloromethane

1 Synthesis

General Information

All commercial reagents (compound **7**, from Alfa Aesar) were used without further purification. Solvents were dried using the appropriate desiccants and distilled prior to use. ^{1}H NMR and ^{13}C NMR were recorded on a Bruker Avance 400 MHz using the deuterated solvent as the lock and residual protiated solvent as the internal reference (CD_2Cl_2: δ_H = 5.32 ppm and δ_C = 53.8 ppm). The following abbreviations were utilized to describe peak patterns: s = singlet, d = doublet, t = triplet, dd = doublet of doublets, td = triplet of doublets, dt = doublet of triplets, br = broad, bs = broad singlet, bd = broad doublet and m = multiplet. The numbering of the carbon atoms in the molecular formulae (*vide infra*) is used only for the assignments of the NMR signals and thus is not necessarily in accordance with IUPAC nomenclature. Electrospray ionization mass spectra (ESI-MS) were recorded on a Thermo-Quest LCQ Deca. UV-vis spectra were recorded on a Cary Win 50 (298 K) spectrometer. Melting points were measured on a Büchi SMP-20 instrument. Infrared spectra were recorded using a Varian 1000 FT-IR instrument. Elemental analysis was done on the EA 3000 CHNS. Ligands **1**,[1] **3**,[2] **4**,[2] **5**,[3] **6**,[4] **8**,[5] **9**[6] were synthesized according to known procedures.

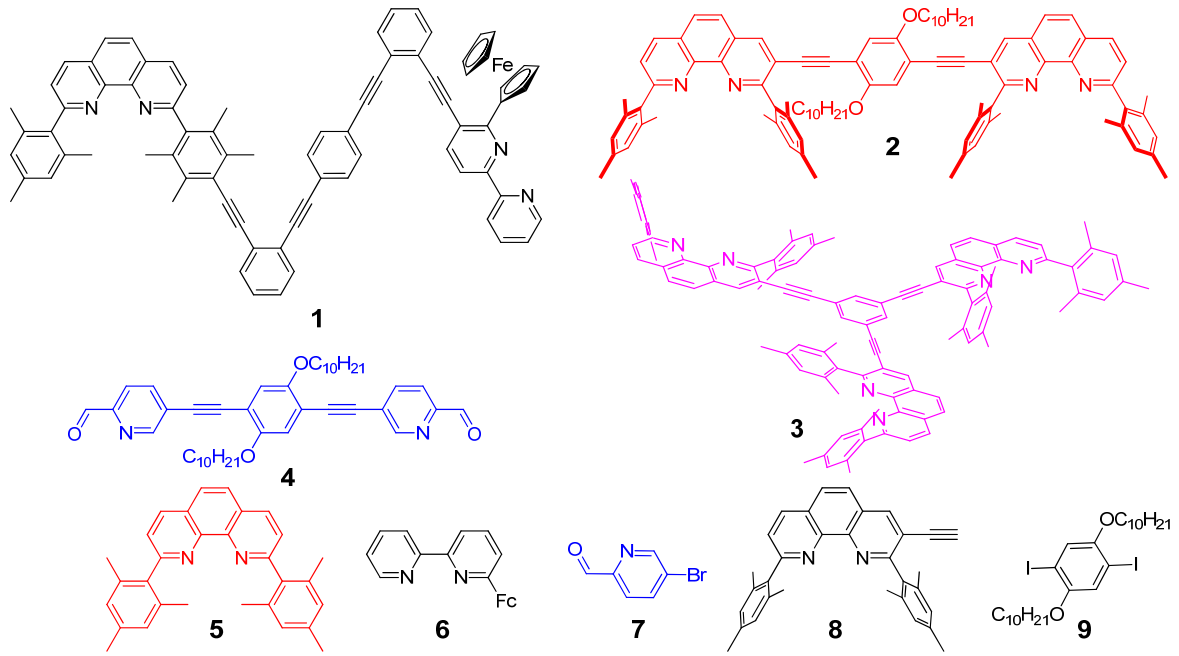

Chart 1: Chemical structures of compounds **1**-**9**.

Synthetic Procedures

Synthesis of ligand 2

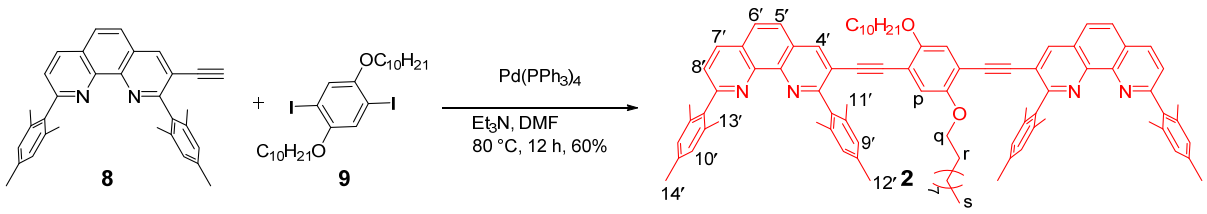

3-Ethynyl-2,9-dimesityl-1,10-phenanthroline (**8,** 50.0 mg, 113 µmol) and 1,4-bis(decyloxy)-2,5-diiodobenzene (**13**, 36.4 mg, 56.7 µmol) were dissolved in a mixture of dry DMF (10 mL) and dry Et_3N (10 mL). The solution was trice subjected to freeze-pump-thaw cycles for removing atmospheric oxygen. Then, $Pd(PPh_3)_4$ (6.55 mg, 5.67 µmol) was added into the mixture under N_2 atmosphere and subjected to heating at 80 °C for overnight. The reaction mixture was then cooled and solvents were evaporated under reduced pressure. The crude mixture was purified by column chromatography eluting with 5% ethyl acetate in *n*-hexane on silica gel (R_f = 0.37, 5% ethyl acetate in *n*-hexane) to furnish a yellow solid in 60% yield. Mp >250 °C. ^{1}H NMR (400 MHz, CD_2Cl_2) δ 8.47 (s, 2H, 4′-H), 8.32 (d, ^3J = 8.0 Hz, 2H, 7′-H), 7.91 (d, ^3J = 8.8 Hz, 2H, [5′/6′]-H), 7.86 (d, ^3J = 8.8 Hz, 2H, [6′/5′]-H), 7.56 (d, ^3J = 8.0 Hz, 2H, 8′-H), 6.98 (s, 4H, [9′/10′]-H), 6.95 (s, 4H, [10′/9′]-H), 6.37 (s, 2H, p-H), 3.85 (t, ^3J = 6.4 Hz, 4H, q-H), 2.35 (s, 6H, [12′/14′]-H), 2.33 (s, 6H, [14′/12′]-H), 2.05 (s, 12H, [11′/13′]-H), 2.04 (s, 12H, [13′/11′]-H), 1.84-1.77 (m, 4H, r-H), 1.59-1.22 (m, 28H, -$(CH_2)_7$-H), 0.82 (t, ^3J = 7.2 Hz, 6H, s-H); ^{13}C NMR (100 MHz, CD_2Cl_2) δ 161.9, 160.9, 153.4, 146.4, 145.4, 138.8, 138.4, 137.8, 137.6, 137.6, 136.4, 136.4, 136.1, 128.6, 128.2, 127.9, 127.3, 127.3, 126.0, 125.1, 120.2, 117.5, 114.1, 92.5, 91.9, 69.8, 32.3, 30.2, 30.0, 29.9, 29.8, 29.6, 26.5, 23.0, 21.4, 21.2, 20.4, 20.1, 14.2; ESI-MS: *m/z* (%) 1267.8 (100) $[M+H]^+$; Anal. Calcd. for $C_{90}H_{98}N_4O_2$: C, 85.27; H, 7.79; N, 4.42; found: C, 84.91; H, 7.75; N, 4.31.

Synthesis[7] of complex [Cu(1)]$^+$

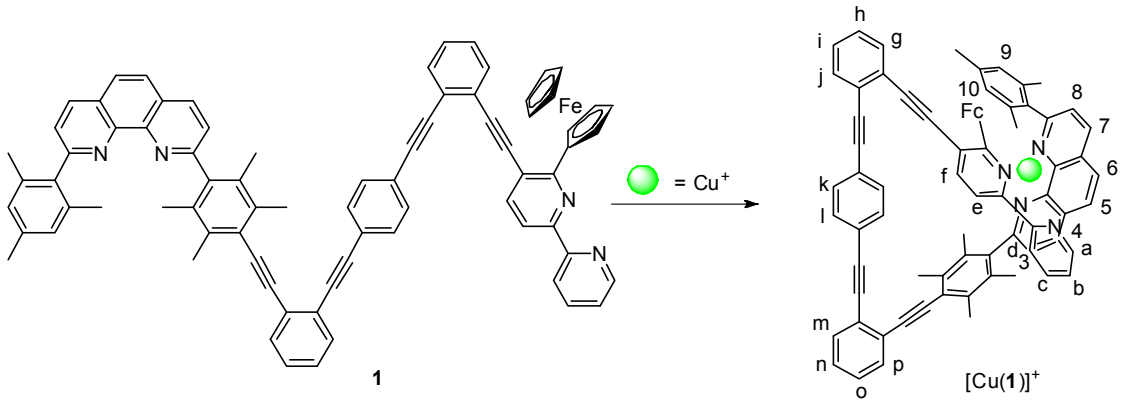

$[Cu(CH_3CN)_4]PF_6$ (123 µg, 0.329 µmol) and molecular switch **1** (360 µg, 0.329 µmol) were taken in a NMR tube directly and dissolved in 500 µL of CD_2Cl_2. The resultant mixture was subjected to analytical characterization without any purification. Yield: Quantitative; ^{1}H NMR (400 MHz, 298 K, CD_2Cl_2): δ = 8.65 (d, ^3J = 8.0 Hz, 1 H, 7/4-H), 8.63 (d, ^3J = 8.0 Hz, 1 H, 4/7-H), 8.19 (s, 2 H, 5-, 6-H), 8.03 (dd, ^3J = 4.6 Hz, ^4J = 1.2 Hz, 1 H, a-H), 7.80 (td, ^3J = 8.0 Hz, ^4J = 1.2 Hz, 1 H, c-H), 7.77 (d, ^3J = 8.4 Hz, 2 H, 3-, 8-H), 7.66-7.72 (m, 3 H, d-, m-, p-H), 7.60-7.64 (m, 3 H, g-, j-, f-H), 7.51 (s, 4 H, k-, l-H), 7.46-7.48 (m, 2 H, n-, o-H), 7.40-7.42 (m, 2 H, h-, i-H), 7.31 (ddd, ^3J = 8.0 Hz, ^3J = 4.8 Hz, ^4J = 1.2 Hz, 1 H, b-H), 7.29 (d, ^3J = 8.4 Hz, 1 H, e-H), 6.43 (s, 1 H, 10/9-H), 6.35 (s, 1 H, 9/10-H), 4.92 (bs, 1 H, Fc-H), 4.54 (bs, 1 H, Fc-H), 3.89 (bs, 5 H, Fc-H), 3.67 (bs, 1 H, Fc-H), 3.32 (bs, 1 H, Fc-H), 2.17 (s, 3 H, duMe-H), 1.97 (s, 3 H, mesMe-H), 1.78 (s, 3 H, mesMe-H), 1.73 (s, 3 H, duMe-H), 1.68 (s, 3 H, duMe-H), 1.65 (s, 3 H, mesMe-H), 1.53 (s, 3 H, duMe-H) ppm.

Synthesis[7] of complex $[Zn(1)_2]^{2+}$

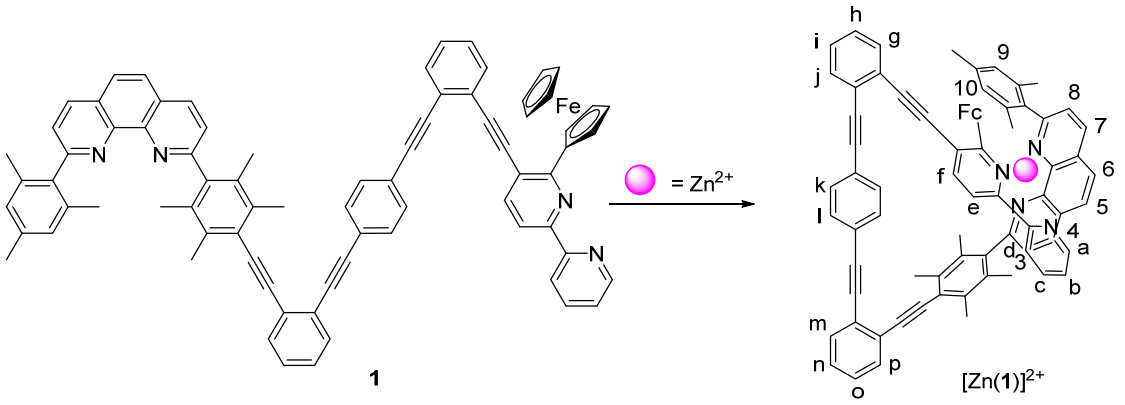

$Zn(OTf)_2$ (271 µg, 0.746 µmol) and molecular switch **1** (816 µg, 0.746 µmol) were placed in a 25 mL flask and refluxed in 15 mL of CH_2Cl_2/CH_3CN = 3:1 for 30 min. After removal of the solvent under reduced pressure the resultant mixture was subjected to analytical characterization without any purification. Yield: Quantitative; ^{1}H NMR (400 MHz, 298 K, CD_2Cl_2: CD_3CN (3:1)): δ = 9.12 (d, ^3J = 8.4 Hz, 1 H, 7/4-H), 8.92 (d, ^3J = 8.4 Hz, 1 H, 4/7-H), 8.71 (d, ^3J = 5.2 Hz, 1 H, a-H), 8.45 (d, ^3J = 8.8 Hz, 1 H, [5/6]-H), 8.39 (d, ^3J = 8.8 Hz, 1 H, [6/5]-H), 8.20 (td, ^3J = 8.0 Hz, ^4J = 1.2 Hz, 1 H, c-H), 8.17 (d, ^3J = 8.4 Hz, 1 H, [3/8]-H), 8.02 (d, ^3J = 8.0 Hz, 1 H, d-H), 7.93 (d, ^3J = 8.4 Hz, 1 H, [8/3]-H), 7.89 (d, ^3J = 8.4 Hz, 1 H, f-H), 7.81-7.83 (m, 1 H, p-H), 7.74 (ddd, ^3J = 7.6 Hz, ^3J = 5.2 Hz, ^4J = 1.2 Hz, 1 H, b-H), 7.67-7.63 (m, 3 H, g-, j-, m-H), 7.62 (s, 4 H, k-, l-H), 7.58 (d, ^3J = 8.4 Hz, 1 H, e-H), 7.56-7.54 (m, 2 H, h-, i-H), 7.46-7.44 (m, 2 H, n-, o-H), 6.43 (s, 1 H, [10/9]-H), 6.03 (s, 1 H, [9/10]-H), 5.48 (bs, 1 H, Fc-H), 4.37 (bs, 1 H, Fc-H), 3.98 (bs, 5 H, Fc-H), 3.84 (bs, 1 H, Fc-H), 3.35 (bs, 1 H, Fc-H), 2.22 (s, 3 H, mesMe-H), 1.89 (s, 3 H, duMe-H), 1.86 (s, 6 H, duMe-H), 1.83 (s, 3 H, mesMe-H), 1.71 (s, 3 H, duMe-H), 1.53 (s, 3 H, mesMe-H) ppm.

Synthesis of rectangle R $[Cu_4(2)_2(4)_2]^{2+}$

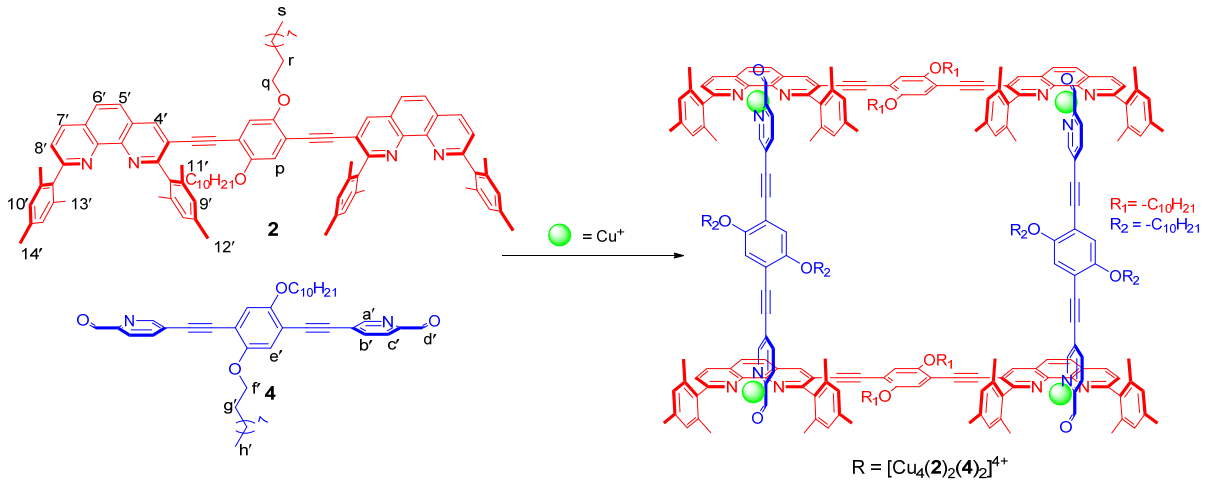

Ligand **2** (667 µg, 0.526 µmol), ligand **4** (341 µg, 0.526 µmol) and $[Cu(CH_3CN)_4]PF_6$ (392 µg, 1.05 µmol) were placed in a 25 mL flask and refluxed in 10 mL of CH_2Cl_2 for 10 min. After removal of the solvent under reduced pressure the resultant mixture was subjected to analytical characterization without any purification. Yield: Quantitative; ^{1}H NMR (400 MHz, 298 K, CD_2Cl_2): δ = 9.52 (s, 4 H, d′-H), 8.75 (s, 4 H, 4′-H), 8.68 (d, ^3J = 8.0 Hz, 4 H, 7′-H), 8.20-8.11 (m, 16 H, a′, b′, 5′ & 6′]-H), 7.90 (d, ^3J = 8.0 Hz, 4 H, 8′-H), 7.75 (d, ^3J = 8.0 Hz, 4 H, c′-H), 7.14 (s, 4 H, e′-H), 6.62 (s, 8 H, [9′/10′]-H), 6.59 (s, 8 H, [10′/9′]-H), 6.35 (s, 4 H, p-H), 4.06 (t, ^3J = 6.4 Hz, 8 H, f′-H), 3.71 (t, ^3J = 6.4 Hz, 8 H, q-H), 2.07 (s, 12 H, [12′/14′]-H), 2.05 (s, 12 H, [14′/12′]-H), 1.93 (s, 24 H, [11′/13′]-H), 1.92 (s, 24 H, [13′/11′]-H), 1.85-1.78 (m, 8 H, r-H), 1.67-1.61 (m, 8 H, g′-H), 1.54-1.17 (m, 112 H, -$(CH_2)_7$&-$(CH_2)_7$-H), 0.84-0.80 (m, 24 H, s& h′-H). ESI-MS: *m/z* (%) = 1022.1 (100) $[Cu_4(\mathbf{2})_2(\mathbf{4})_2]^{4+}$, 1411.2 (40) $[Cu_4(\mathbf{2})_2(\mathbf{4})_2](PF_6)^{3+}$.

Synthesis of prism P $[Cu_6(3)_2(4)_3]^{6+}$

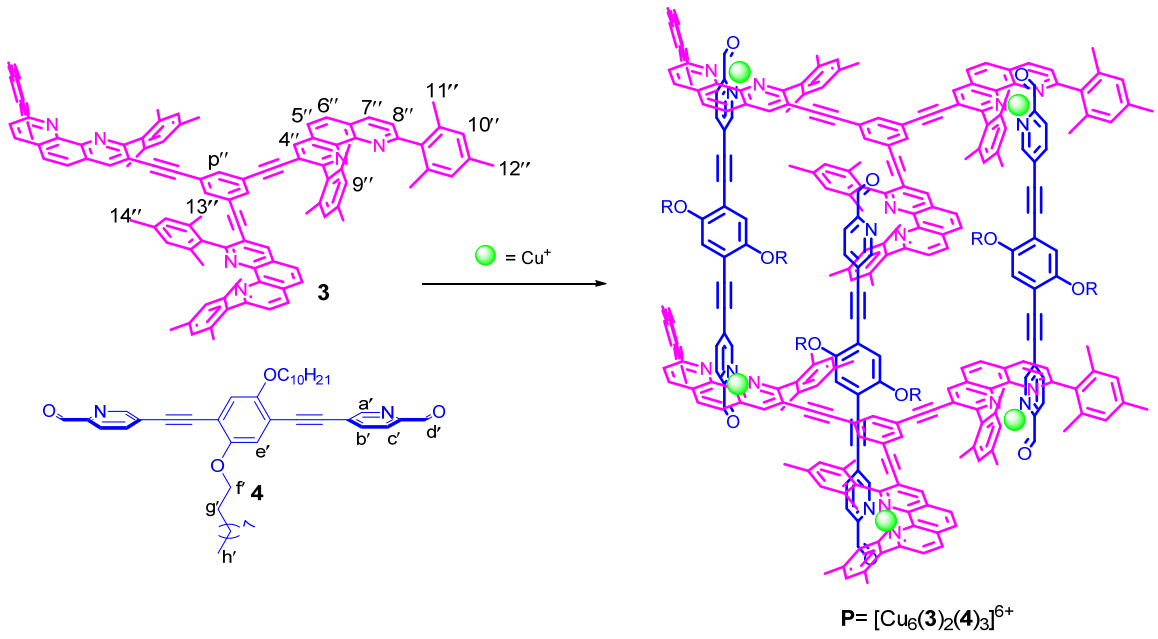

Ligand **3** (667 µg, 0.526 µmol), ligand **4** (341 µg, 0.526 µmol) and $[Cu(CH_3CN)_4]PF_6$ (392 µg, 1.05 µmol) were placed in a 25 mL flask and refluxed in 10 mL of CH_2Cl_2 for 10 min. After removal of the solvent under reduced pressure the resultant mixture was subjected to analytical characterization without any purification. Yield: Quantitative; ^{1}H NMR (400 MHz, 298 K, CD_2Cl_2): δ = 9.57 (brs, 6 H, d′-H), 8.77 (s, 6 H, 4″-H), 8.70 (d, ^3J = 8.4 Hz, 6 H, 7″-H), 8.22 (brs, 18 H, a′, 5″ & 6″-H), 8.13 (brd, ^3J = 8.0 Hz, 6 H, b′-H), 7.91 (d, ^3J = 8.4 Hz, 6 H, 8″-H), 7.81 (d, ^3J = 8.0 Hz, 6 H, c′-H), 7.11 (s, 6 H, e′-H), 6.63 (brs, 30 H, p″-, 9″- &10″-H), 4.03 (t, ^3J = 6.4 Hz, 12 H, f′-H), 2.14 (s, 18 H, [12′/14′]-H), 2.07 (s, 18 H, [14′/12′]-H), 1.94 (s, 36 H, [11′/13′]-H), 1.88 (s, 36 H, [13′/11′]-H), 1.81-1.75 (m, 12 H, g′-H), 1.53-1.40 (m, 12 H, 3×CH_2-H), 1.27-1.12 (m, 72 H, -$(CH_2)_6$-H), 0.78 (t, ^3J = 7.2 Hz, 18 H, h′-H). ESI-MS: *m*/*z* (%) = 1350.9 (100) $[Cu_6(\mathbf{3})_2(\mathbf{4})_3](PF_6)_2^{4+}$, 1850.3 (30) $[Cu_6(\mathbf{3})_2(\mathbf{4})_2](PF_6)_3^{3+}$.

2 Regulation of Supramolecular Assemblies by Signaling

Assembly and disassembly of rectangle R by nanoswitch 1

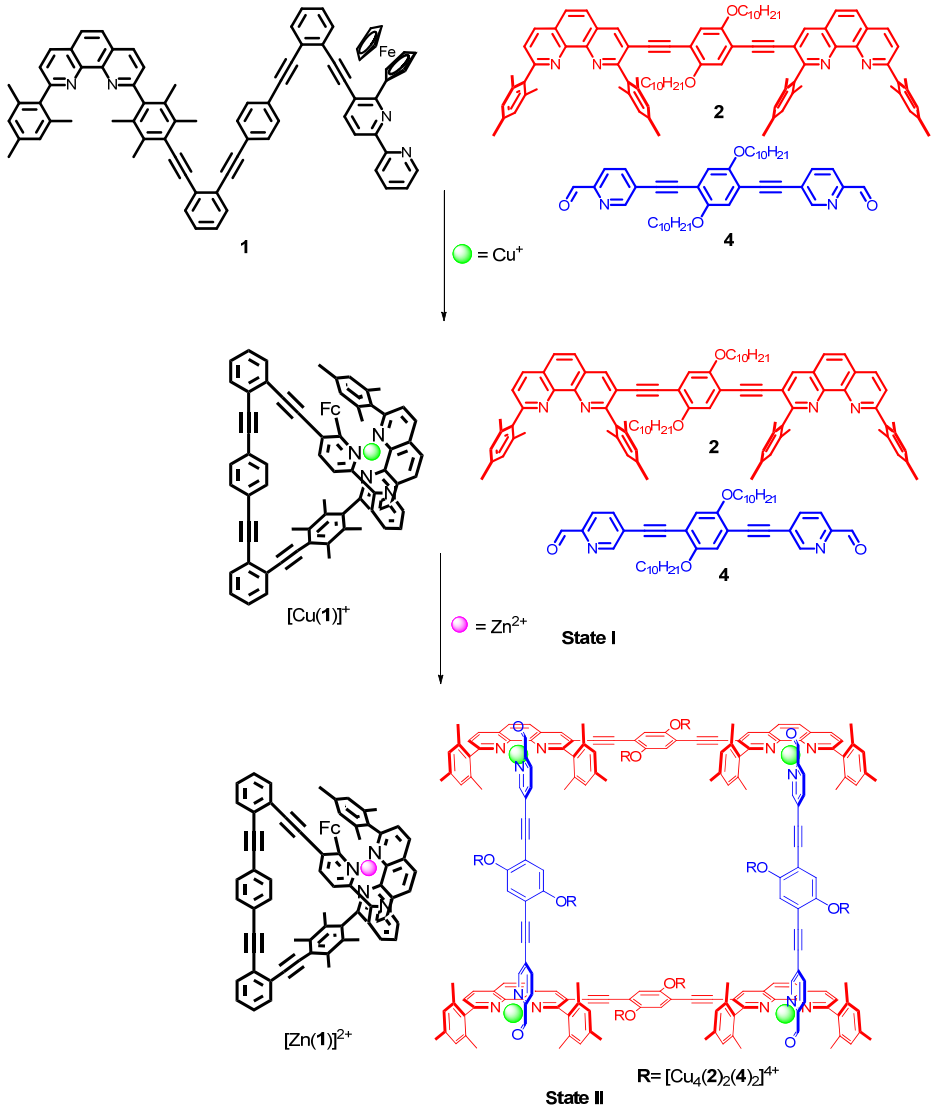

Preparation of state I:

$[Cu(CH_3CN)_4]PF_6$ (271 µg, 0.727 µmol) was added to the solution of nanoswitch **1** (795 µg, 0.727 µmol), ligand **2** (461 µg, 0.364 µmol) and ligand **4** (236 µg, 0.364 µmol) in CD_2Cl_2 (0.5 mL) in an NMR tube. The mixture was sonicated for 2-3 min to afford a clear reddish orange solution. ^1H NMR analysis of the mixture clearly showed that Cu^+ was bound to nanoswitch **1** while ligand **2** and ligand **4** remained free in the solution (see Figures S12 and S13).

Preparation of state II:

$Zn(OTf)_2$ (171 μg, 0.471 μmol) dissolved in 1.0 mL of CH_3CN was added into the solution of nanoswitch **1** (515 μg, 0.471 μmol) in 9.0 mL of CH_2Cl_2. After stirring for 2-3 min, ligand **2** (299 μg, 0.235 μmol), ligand **4** (153 μg, 0.235 μmol) and $[Cu(CH_3CN)_4]PF_6$ (176 μg, 0.471 μmol) were added into the same flask. After heating for 30 more min at 60 °C, the solvents were evaporated under reduced pressure and the sample was subjected to ^1H NMR measurement in CD_2Cl_2 without any further purification. Analysis of ^1H NMR confirmed the formation of state II, i.e. 4 × [Zn(**1**)](OTf)$_2$ + [Cu$_4$(**2**)$_2$(**4**)$_2$](PF$_6$)$_4$ (see Figures S14 and S15).

***Insitu* Switching studies (Fig. S16):**

In an NMR tube, nanoswitch **1** (660 μg, 0.604 μmol), ligand **2** (383 μg, 0.302 μmol), ligand **4** (196 μg, 0.302 μmol) and $[Cu(CH_3CN)_4]PF_6$ (225 μg, 0.604 μmol) were dissolved in 500 μL of CD_2Cl_2. After formation of a clear solution the sample was subjected to NMR measurement (see Figure S16d).

After the measurement, $Zn(OTf)_2$ (219 μg, 0.604 μmol) dissolved in 200 μL acetonitrile was added to the sample and was subjected to heating at 60 °C for 30 min. The NMR measurement was done for the sample without any further purification (see Figure S16e).

To check the reversibility of the system, finally hexacyclen (156 μg, 0.604 μmol) was added into the same sample that was heated at 60 °C for 10 min (in a thermostat). Thereafter, the sample was cooled to room temperature and the ^1H NMR spectrum was recorded (See Figure S16f).

Assembly and disassembly of Prism P by Nanoswitch 1

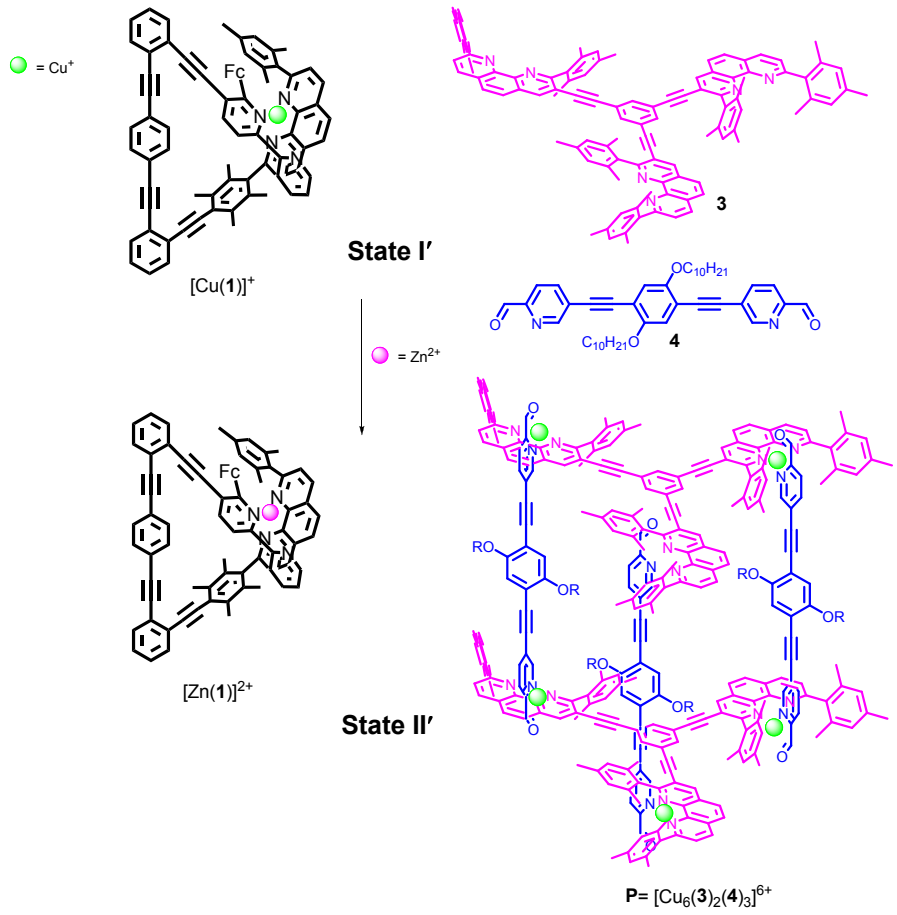

In an NMR tube nanoswitch, **1** (568 µg, 0.520 µmol), ligand **3** (241 µg, 0.173 µmol), ligand **4** (168 µg, 0.260 µmol) and $[Cu(CH_3CN)_4]PF_6$ (194 µg, 0.520 µmol) were dissolved in 500 µL of CD_2Cl_2. The ensuing clear solution was subjected to NMR measurement (see Figure S21d).

After the measurement, $Zn(OTf)_2$ (189 µg, 0.520 µmol), dissolved in 200 µL acetonitrile, was added to the sample that was subjected to heating at 60 °C for 30 min. The NMR measurement was taken without any further purification (see Figure S21e).

To check the reversibility of the system, finally hexacyclen (134 µg, 0.520 µmol) was added into the same sample that was heated at 60 °C for 10 min (in a thermostat). Thereafter, the sample was cooled to room temperature and the ^{1}H NMR spectrum was recorded (See Figure S21f).

3 ^{1}H & ^{13}C NMR Spectra

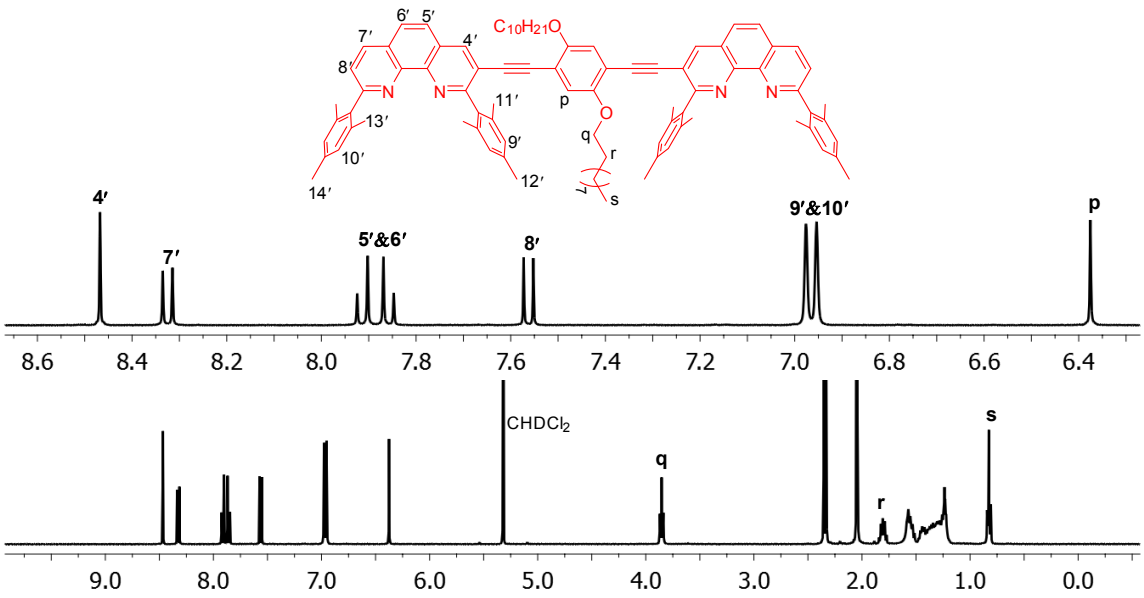

Figure S1: ^{1}H NMR spectrum (400 MHz, CD_2Cl_2, 298 K) of compound **2**. An expanded part of the aromatic region is shown at the top with characteristic protons assigned.

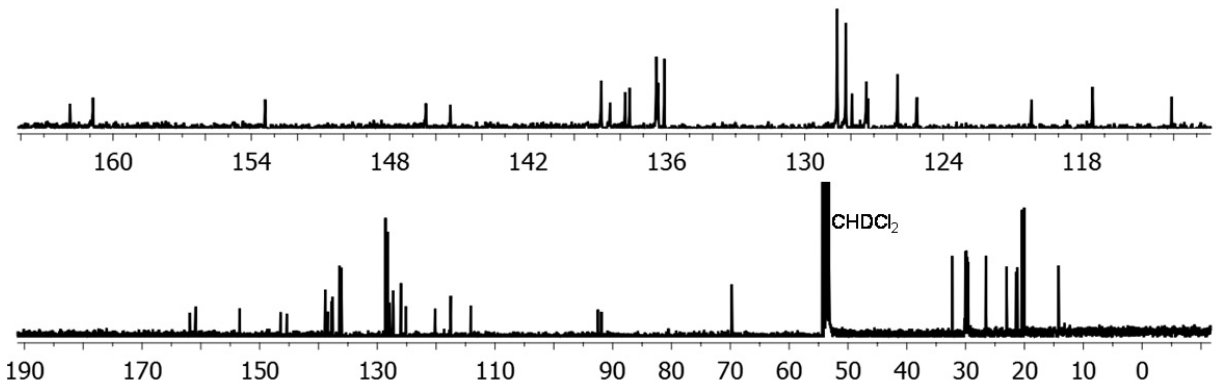

Figure S2: ^{13}C NMR spectrum (100 MHz, CD_2Cl_2, 298 K) of compound **2**. An expanded part of the aromatic region is shown at the top.

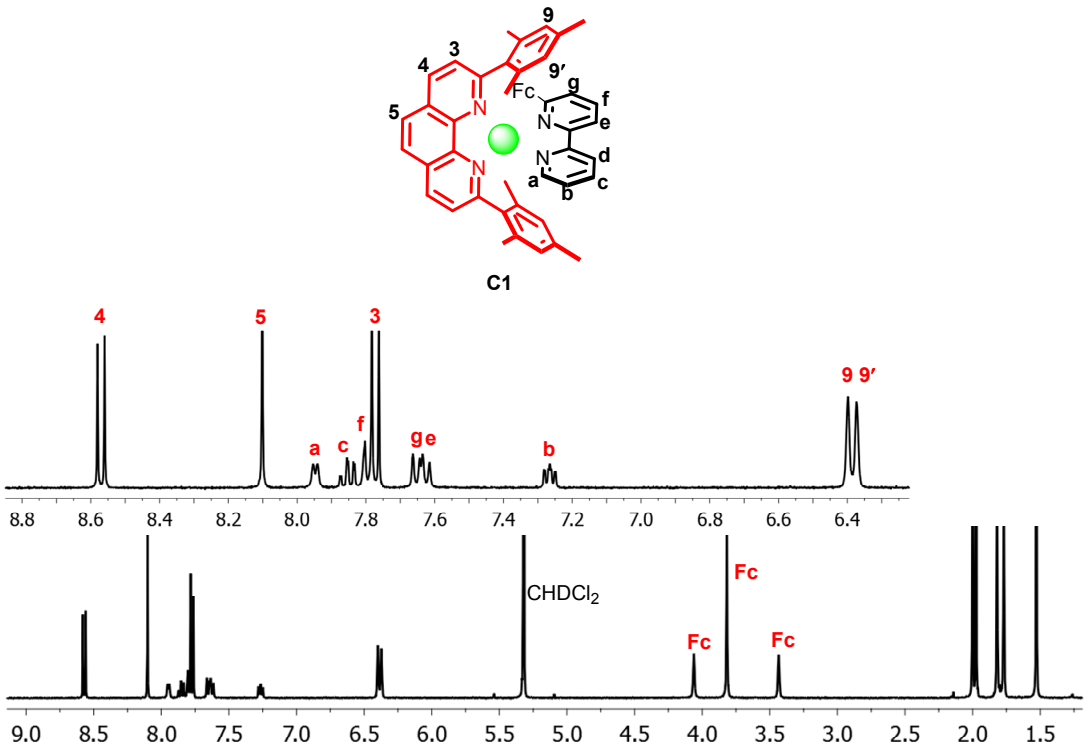

Figure S3: ^{1}H NMR spectrum (400 MHz, CD_2Cl_2, 298 K) of complex **C1** = [Cu(**5**)(**6**)]PF_6. An expanded part of the aromatic region is shown at the top with characteristic protons assigned.

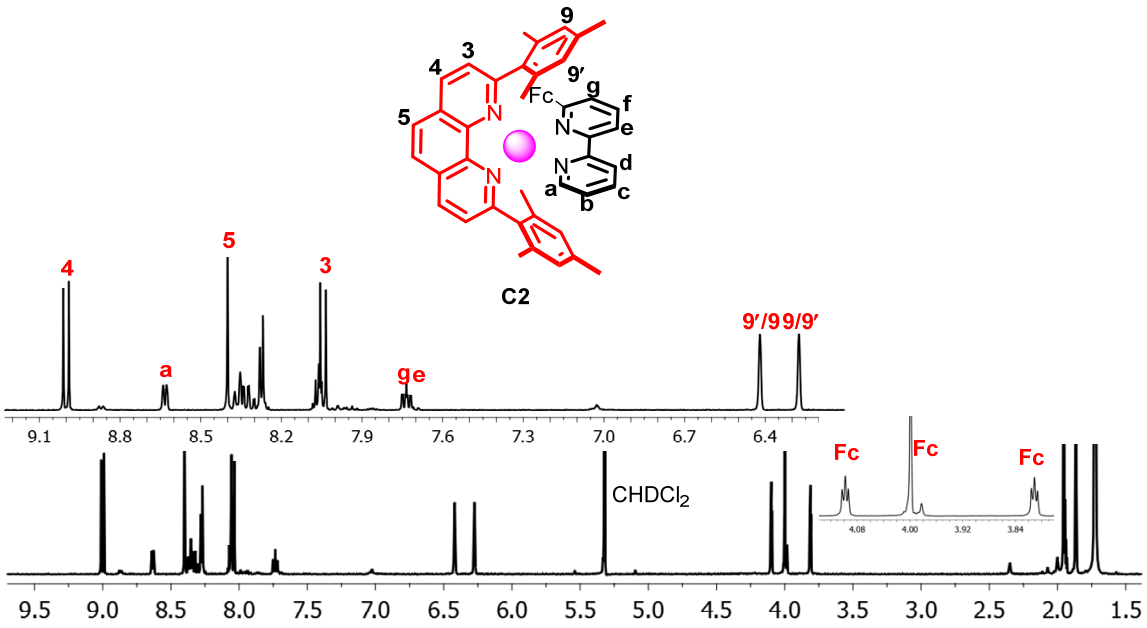

Figure S4: ^{1}H NMR spectrum (400 MHz, CD_2Cl_2, 298 K) of complex **C2** = [Zn(**5**)(**6**)](OTf)$_2$. An expanded part of the aromatic region is shown at the top with characteristic protons assigned.

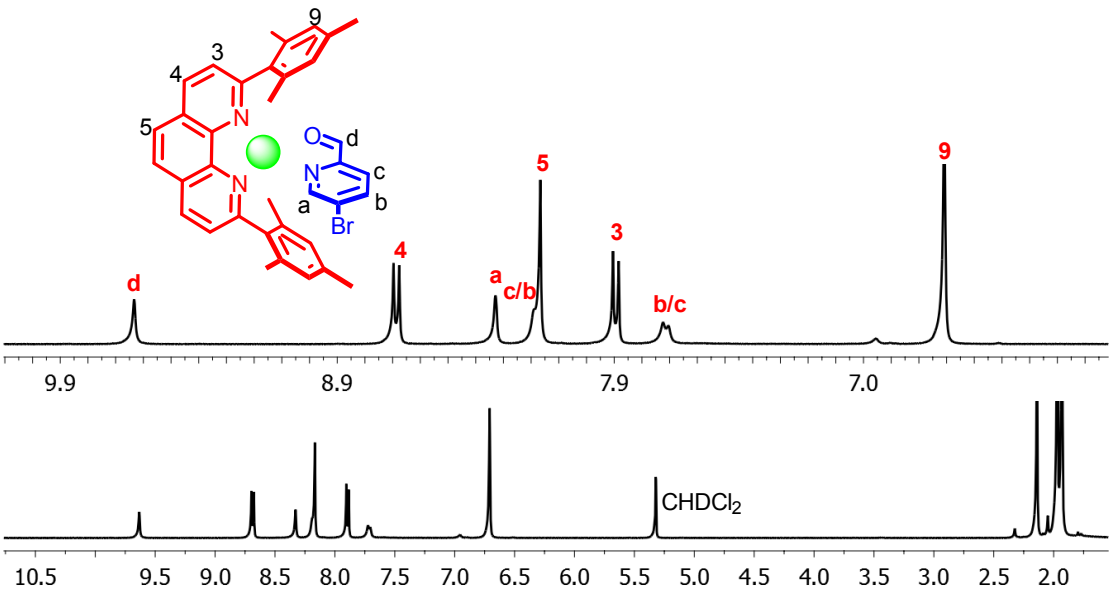

Figure S5: ^{1}H NMR spectrum (400 MHz, CD_2Cl_2, 298 K) of complex **C3** = [Cu(**5**)(**7**)]PF_6. An expanded part of the aromatic region is shown at the top with characteristic protons assigned.

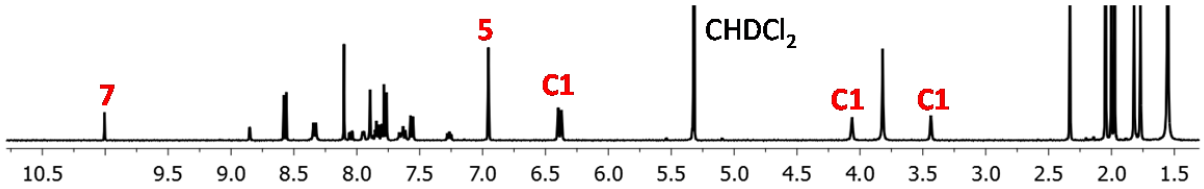

Figure S6: ^{1}H NMR spectrum (400 MHz, CD_2Cl_2, 298 K) of the mixture of ligand **5**, **6**, **7** and $[Cu(CH_3CN)_4]PF_6$ in 2:1:1:1 ratio to form complex **C1** = $[Cu(\mathbf{5})(\mathbf{6})]^{+}$ with 1 equiv. of ligand **5** and **7** free in the solution.

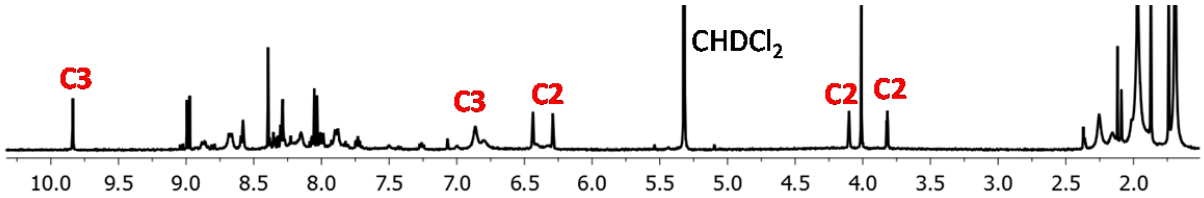

Figure S7: ^{1}H NMR spectrum (400 MHz, CD_2Cl_2, 298 K) of mixture of ligand **5**, **6**, **7**, $[Cu(CH_3CN)_4]PF_6$ and $Zn(OTf)_2$ in 2:1:1:1:1 ratio to form complex **C2** = $[Zn(\mathbf{5})(\mathbf{6})]^{2+}$ and **C3** =$[Cu(\mathbf{5})(\mathbf{7})]^{+}$.

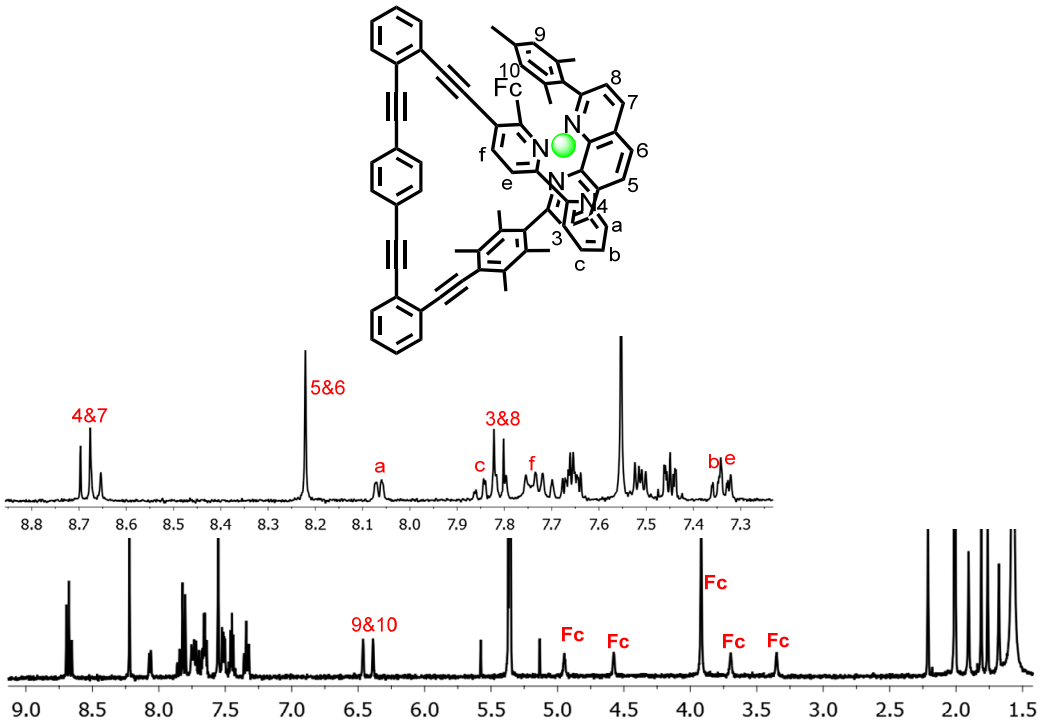

Figure S8: ^{1}H NMR spectrum (400 MHz, CD_2Cl_2, 298 K) of complex [Cu(**1**)]PF_6. An expanded part of the aromatic region is shown at the top with a few characteristic protons assigned.

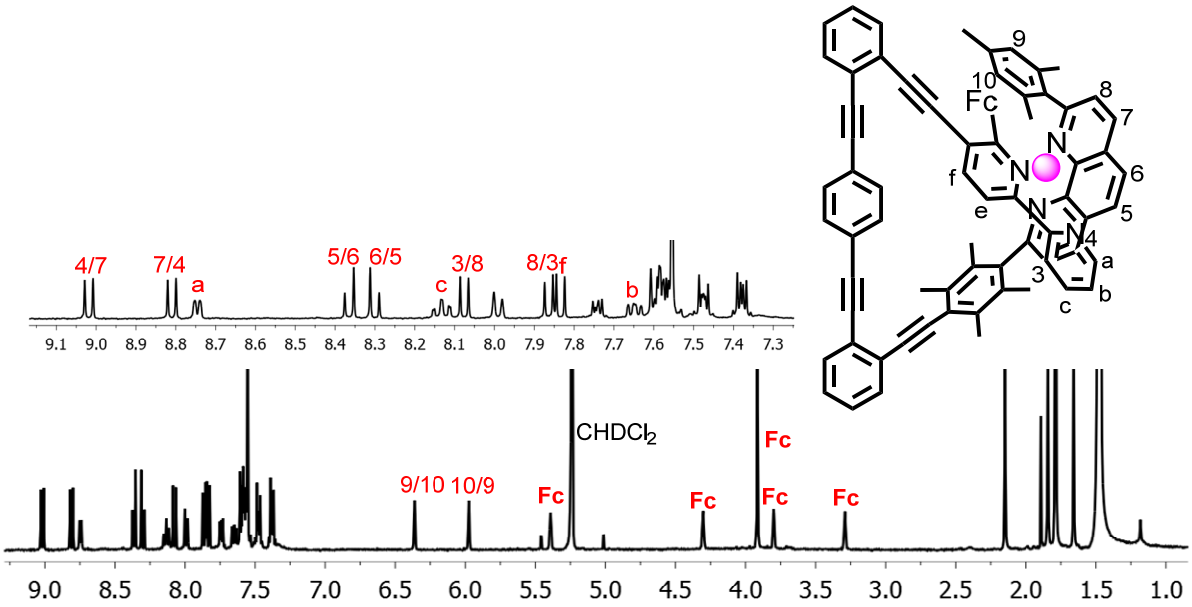

Figure S9: ^{1}H NMR spectrum (400 MHz, CD_2Cl_2, 298 K) of complex [Zn(**1**)]$(OTf)_2$. An expanded part of the aromatic region is shown at the top with a few characteristic protons assigned.

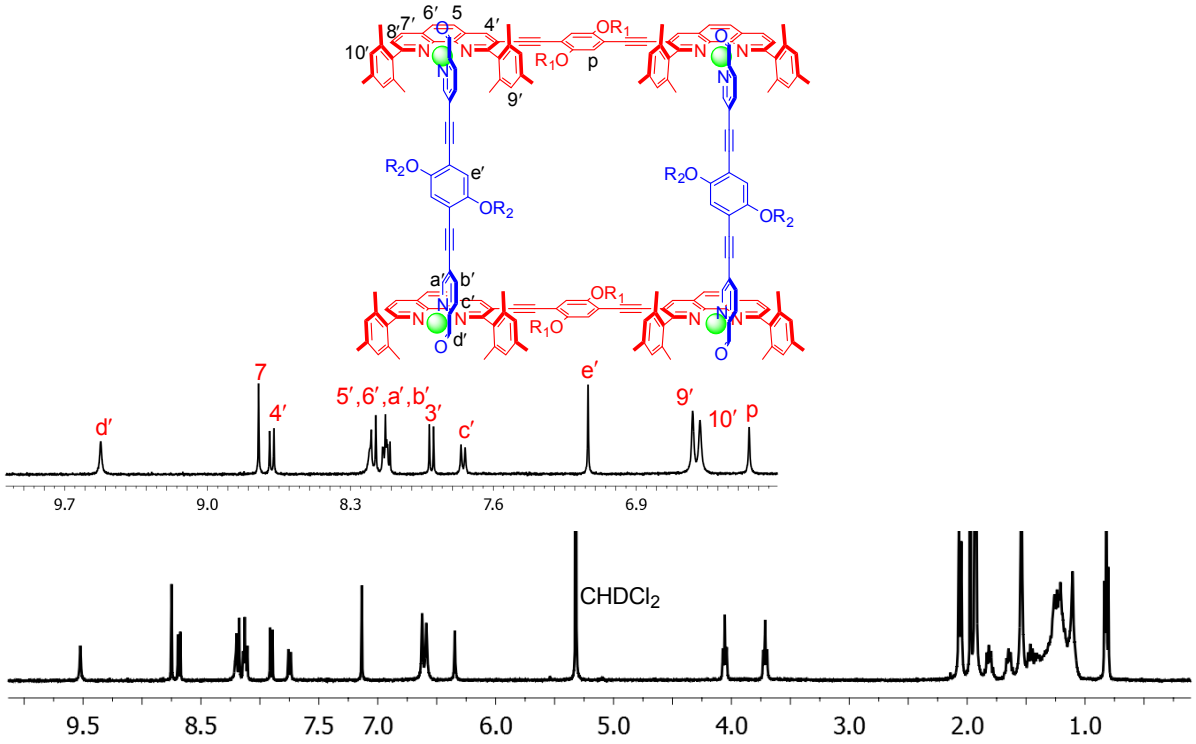

Figure S10: ^{1}H NMR spectrum (400 MHz, CD_2Cl_2, 298 K) of 2D rectangle **R** = $[Cu_4(\mathbf{2})_2(\mathbf{4})_2](PF_6)_4$. An expanded part of the aromatic region is shown at the top with few characteristic protons assigned.

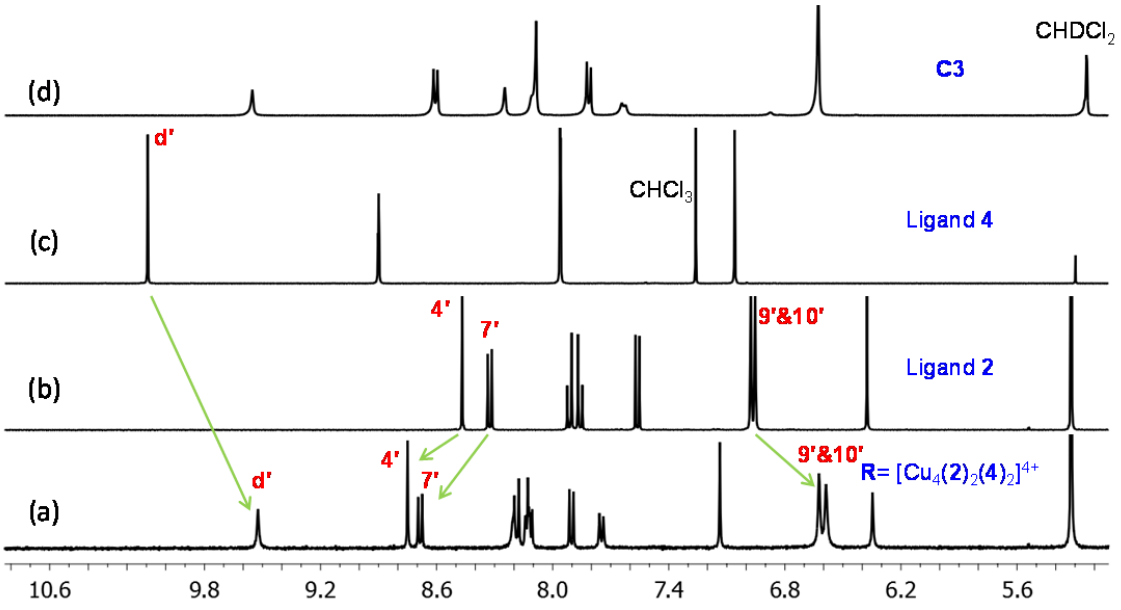

Figure S11: Partial ^{1}H NMR spectra for comparison (400 MHz, CD_2Cl_2, 298 K) of (a) 2D macrocycle **R** = $[Cu_4(\mathbf{2})_2(\mathbf{4})_2]^{4+}$, (b) ligand **2**, (c) ligand **4** and (d) prototypical complex **C3** = $[Cu(\mathbf{5})(\mathbf{7})]^{+}$.

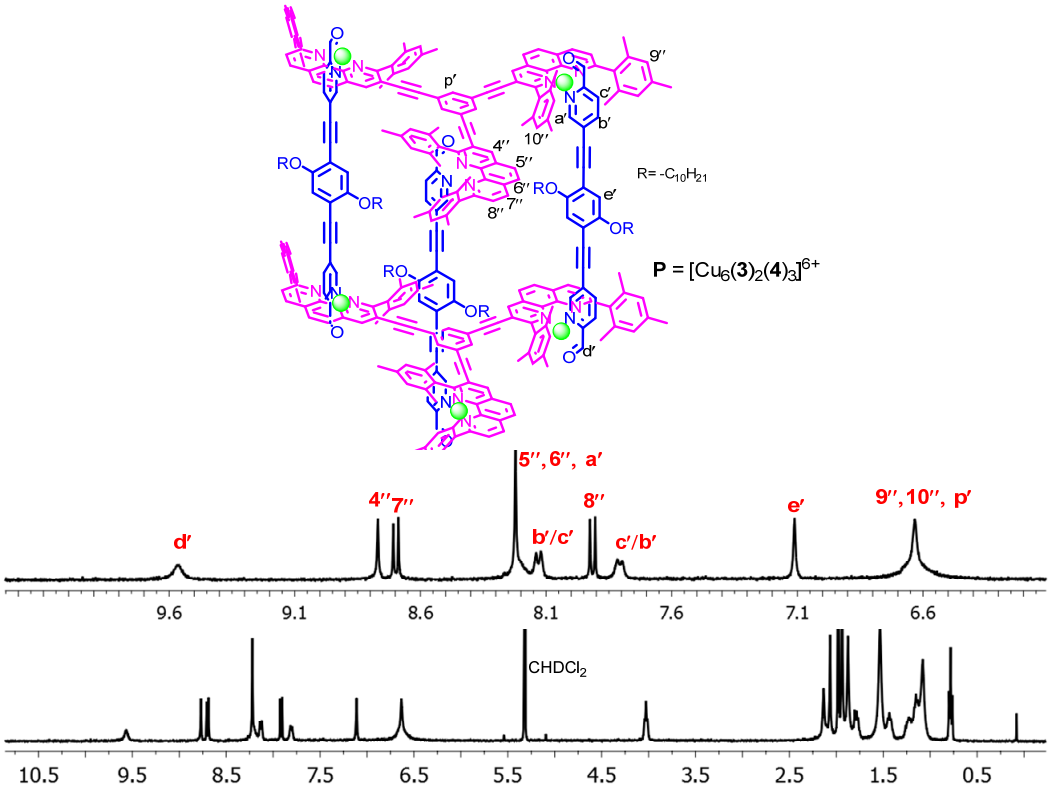

Figure S12: ^{1}H NMR spectrum (400 MHz, CD_2Cl_2, 298 K) of prism **P**= $[Cu_6(\mathbf{3})_2(\mathbf{4})_3](PF_6)_6$. An expanded part of the aromatic region is shown at the top with characteristic protons assigned.

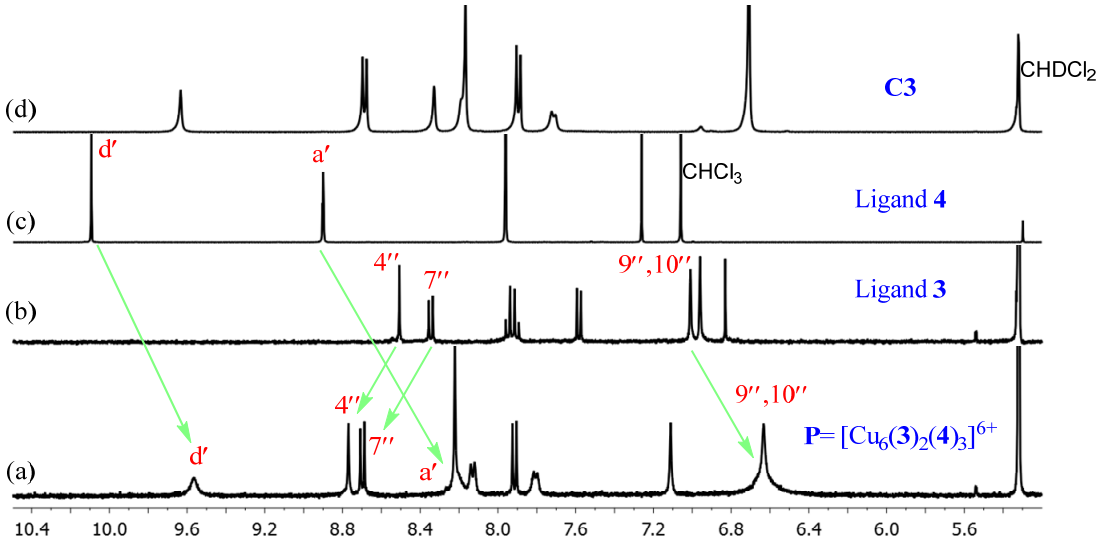

Figure S13: Partial ^{1}H NMR spectra for comparison (400 MHz, CD_2Cl_2, 298 K) of (a) prism **P** = $[Cu_6(\mathbf{3})_2(\mathbf{4})_3]^{6+}$, (b) ligand **3**, (c) ligand **4** and (d) prototypical complex **C3** = $[Cu(\mathbf{5})(\mathbf{7})]^{+}$.

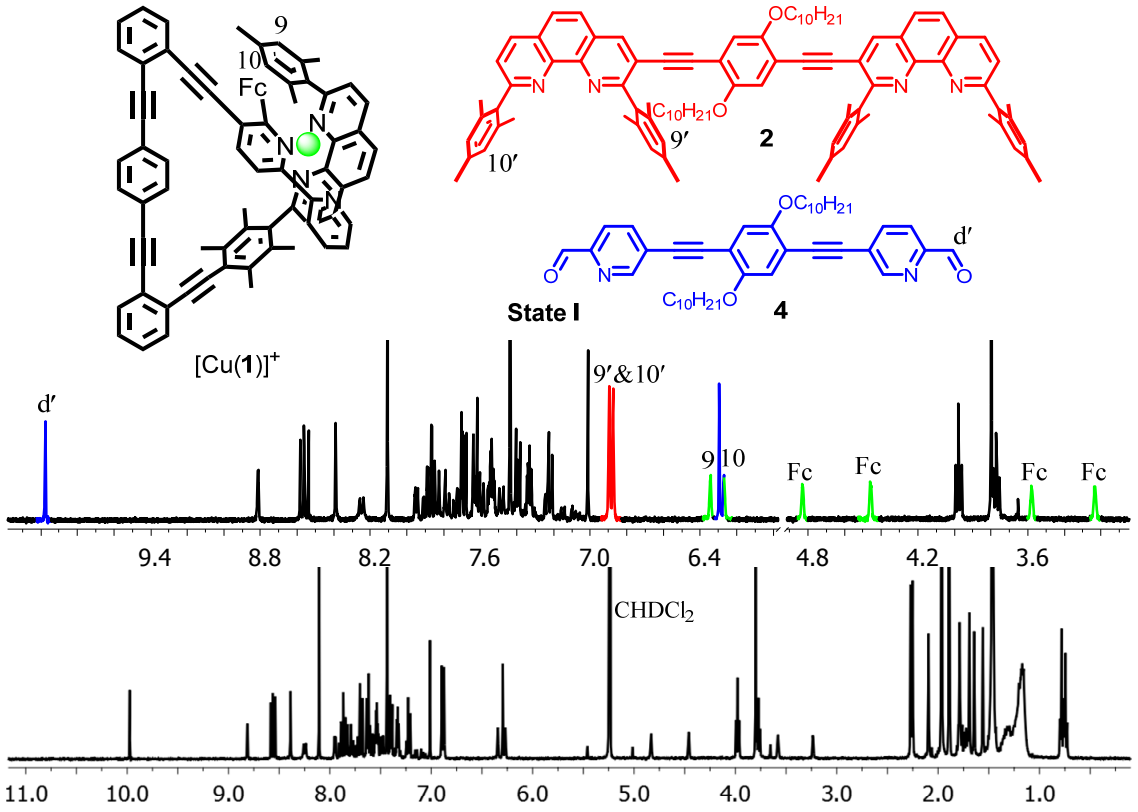

Figure S14: ^{1}H NMR spectra (400 MHz, CD_2Cl_2, 298 K) of State I = 2 × [Cu(**1**)]$^{+}$ + **2** + **4**. An expanded part of the aromatic region is shown at the top with characteristic protons assigned.

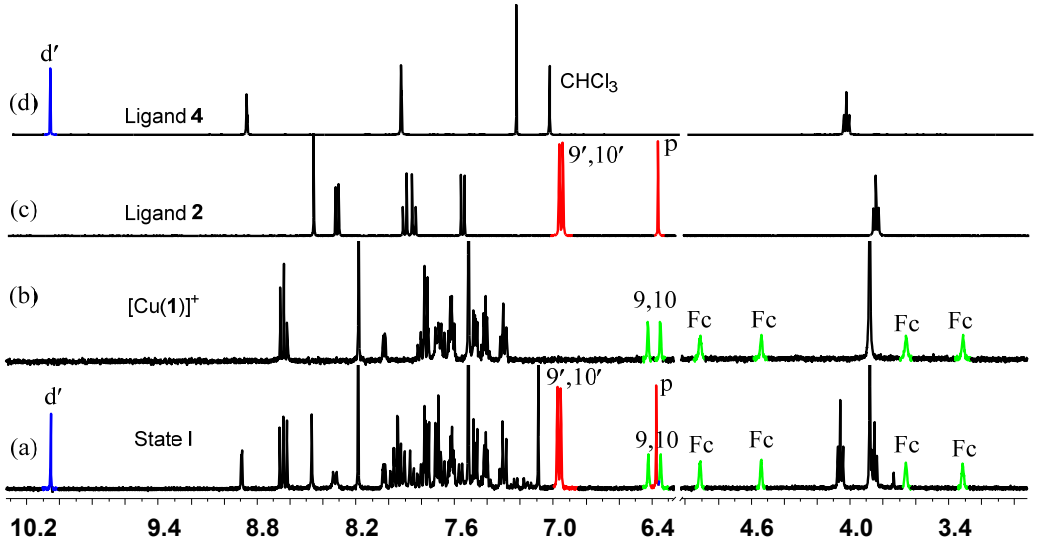

Figure S15: Partial ^{1}H NMR spectra for comparison (400 MHz, CD_2Cl_2, 298 K) of (a) State I, (b) [Cu(**1**)]$^{+}$, (c) ligand **2** and (d) ligand **4**.

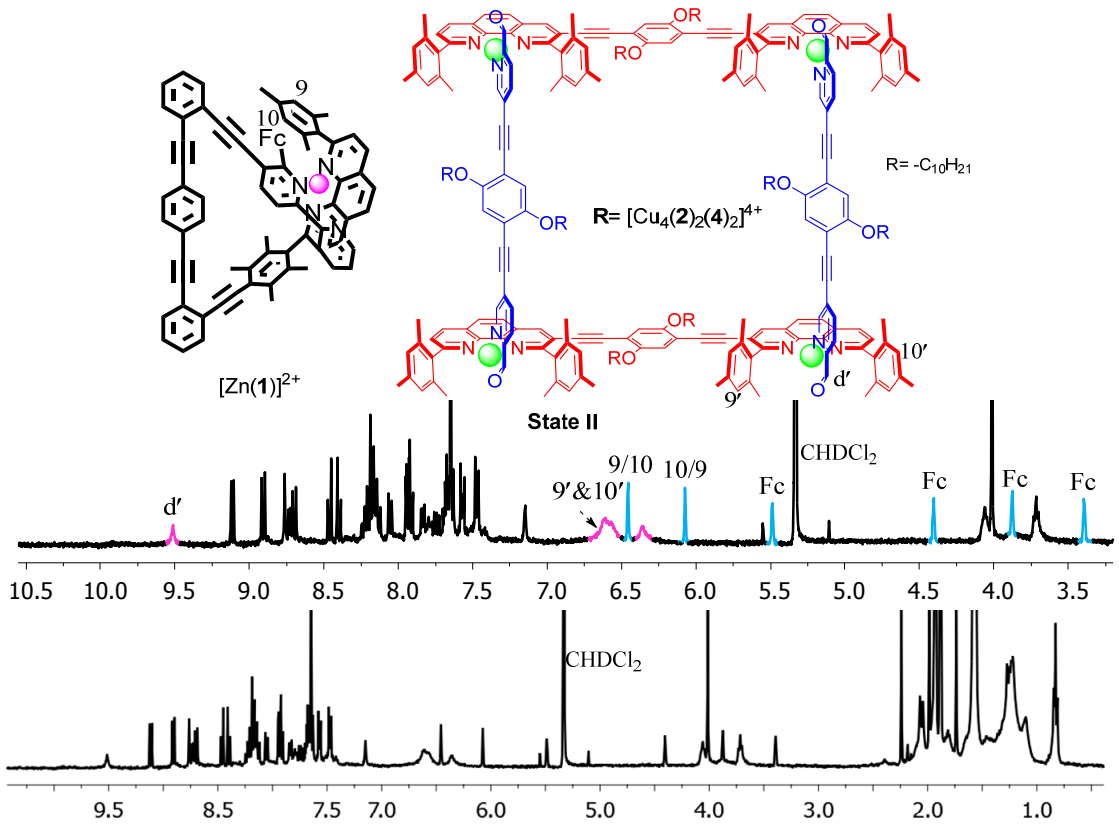

Figure S16: ^{1}H NMR spectra (400 MHz, CD_2Cl_2, 298 K) of State II = 4 × $[Zn(\mathbf{1})]^{2+}$ + $[Cu_4(\mathbf{2})_2(\mathbf{4})_2]^{4+}$. An expanded part of the aromatic region is shown at the top with characteristic protons assigned.

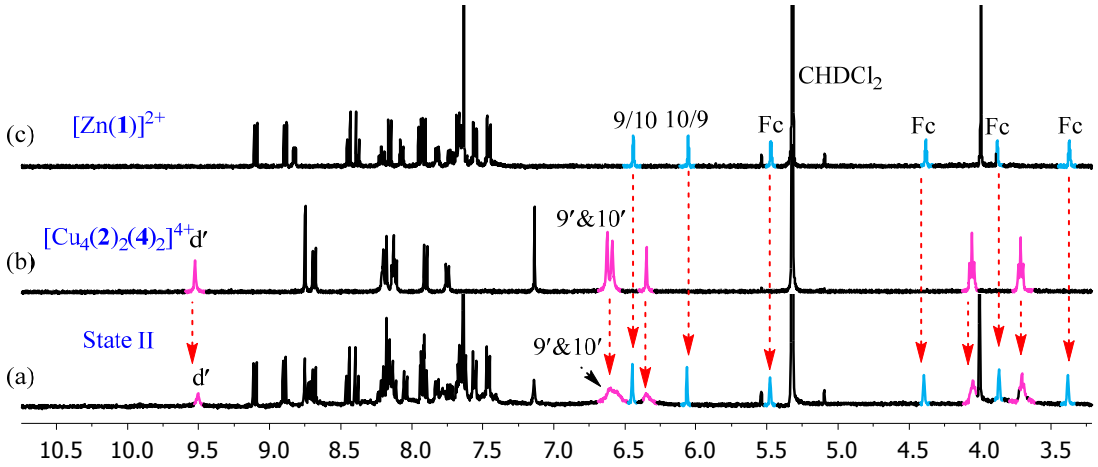

Figure S17: Partial ^{1}H NMR spectra for comparison (400 MHz, CD_2Cl_2, 298 K) of (a) State II, (b) $[Cu_2(\mathbf{2})_2(\mathbf{4})_2]^{4+}$, (c) $[Zn(\mathbf{1})]^{2+}$.

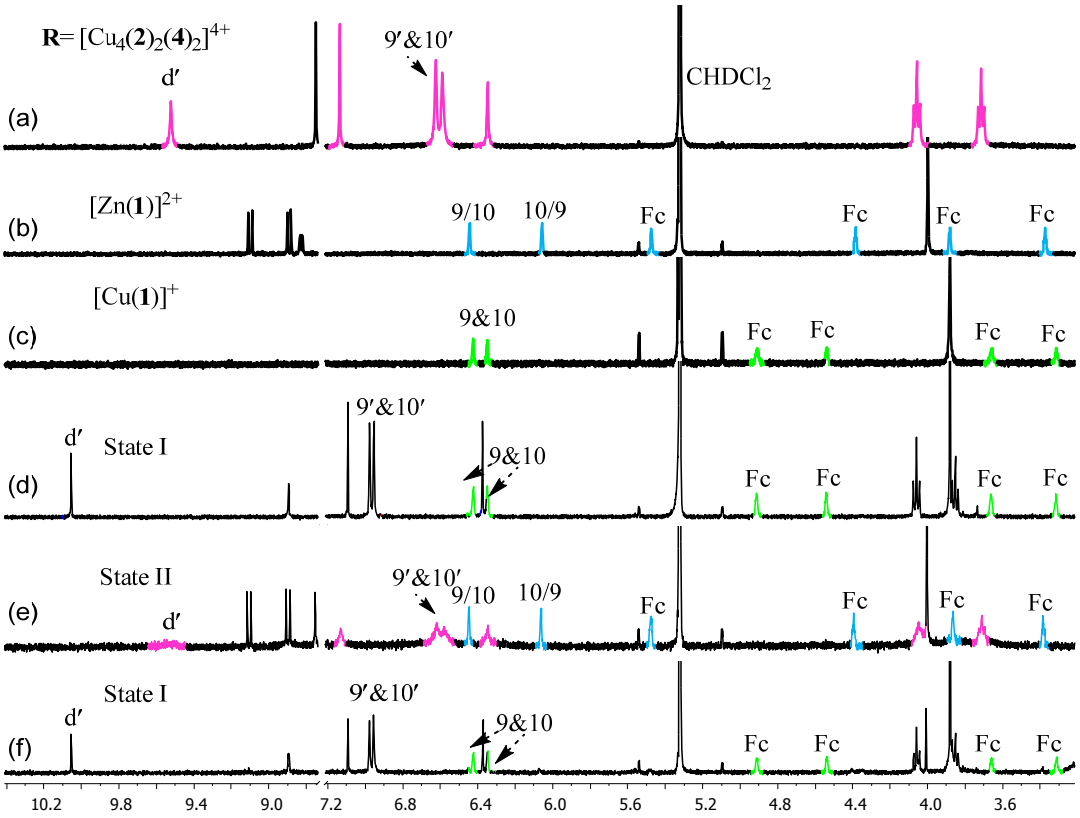

Figure S18: ^{1}H NMR (400 MHz, 298 K, CD_2Cl_2) showing the *in-situ* reversible assembly and disassembly of rectangle **R** by nanoswitch **1**. (a) **R** = $[Cu_4(\mathbf{2})_2(\mathbf{4})_2](PF_6)_4$; (b) $[Zn(\mathbf{1})]^{2+}$; (c) $[Cu(\mathbf{1})]^{+}$; (d) nanoswitch **1**, ligand **2**, **4** and $[Cu(CH_3CN)_4]PF_6$ were mixed in 4:2:2:4 ratio affording state I; (e) addition of 4 equiv. $Zn(OTf)_2$ to state I depicted in spectrum (a) generated state II, i.e. $[Zn(\mathbf{1})]^{2+}$ + $[Cu_4(\mathbf{2})_2(\mathbf{4})_2]^{4+}$; (f) addition of 4 equiv. of hexacyclen to remove Zn^{2+}, regenerated state I along with complex $[Zn(hexacyclen)]^{2+}$.

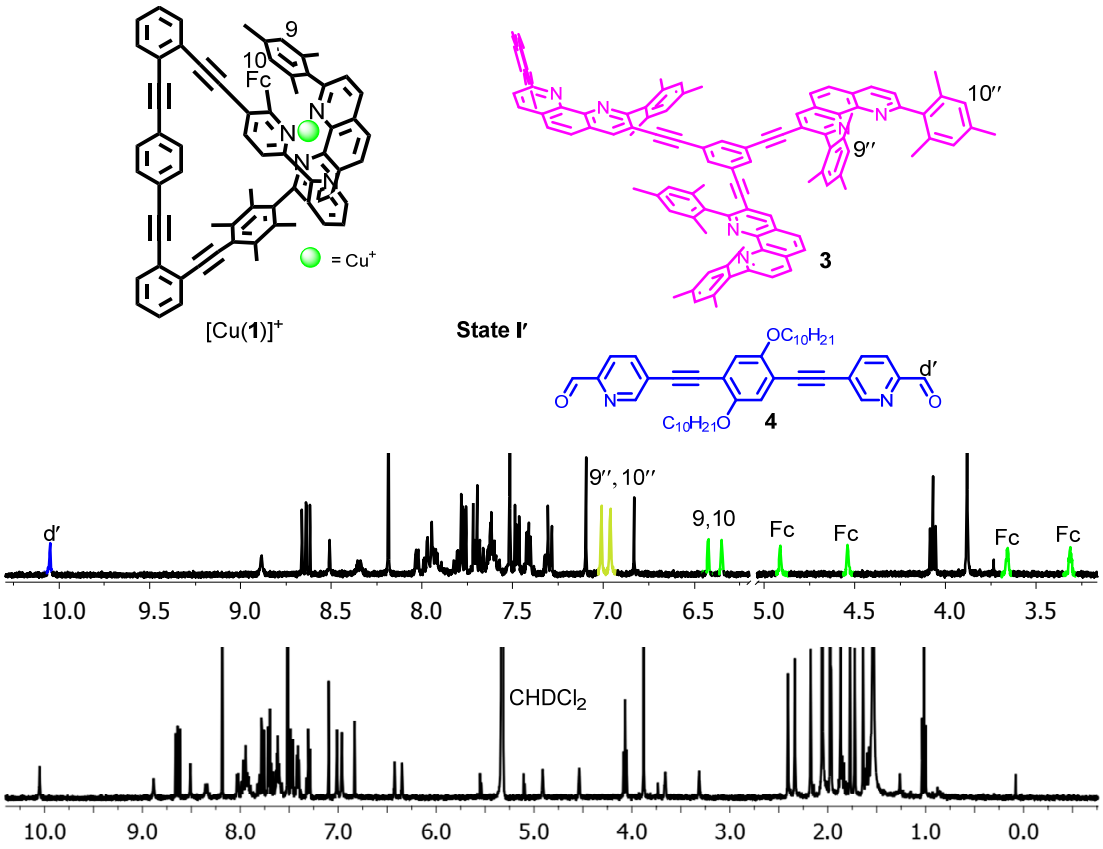

Figure S19: ^{1}H NMR spectra (400 MHz, CD_2Cl_2, 298 K) of State I′ = 6 × [Cu(**1**)]$^{+}$+ 2×**3**+3×**4**. An expanded part of the aromatic region is shown at the top with characteristic protons assigned.

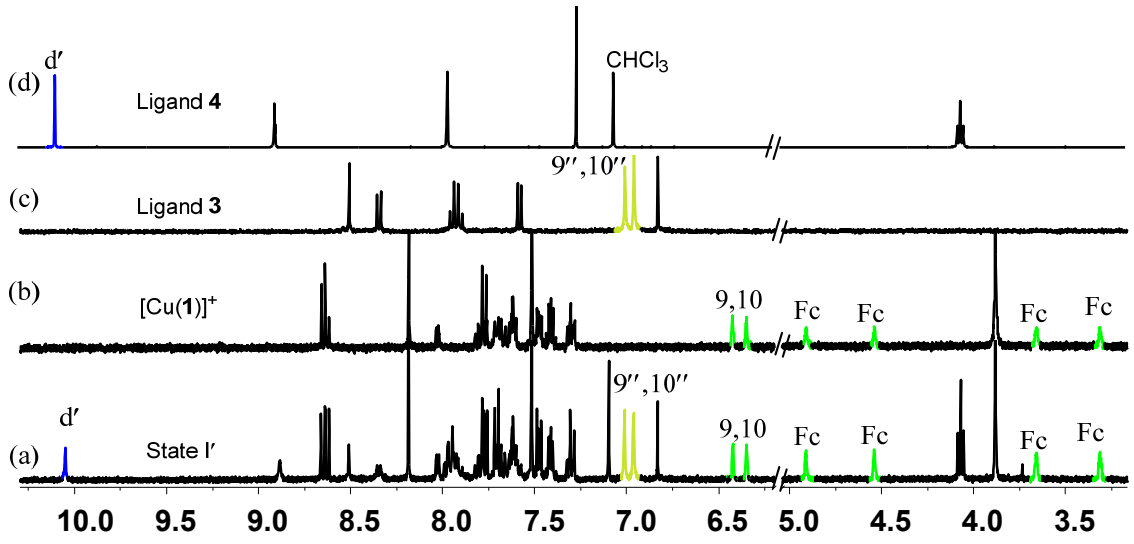

Figure S 20: Partial ^{1}H NMR spectra for comparison (400 MHz, CD_2Cl_2, 298 K) of (a) State I′, (b) [Cu(**1**)]$^{+}$, (c) ligand **3** and (d) ligand **4**.

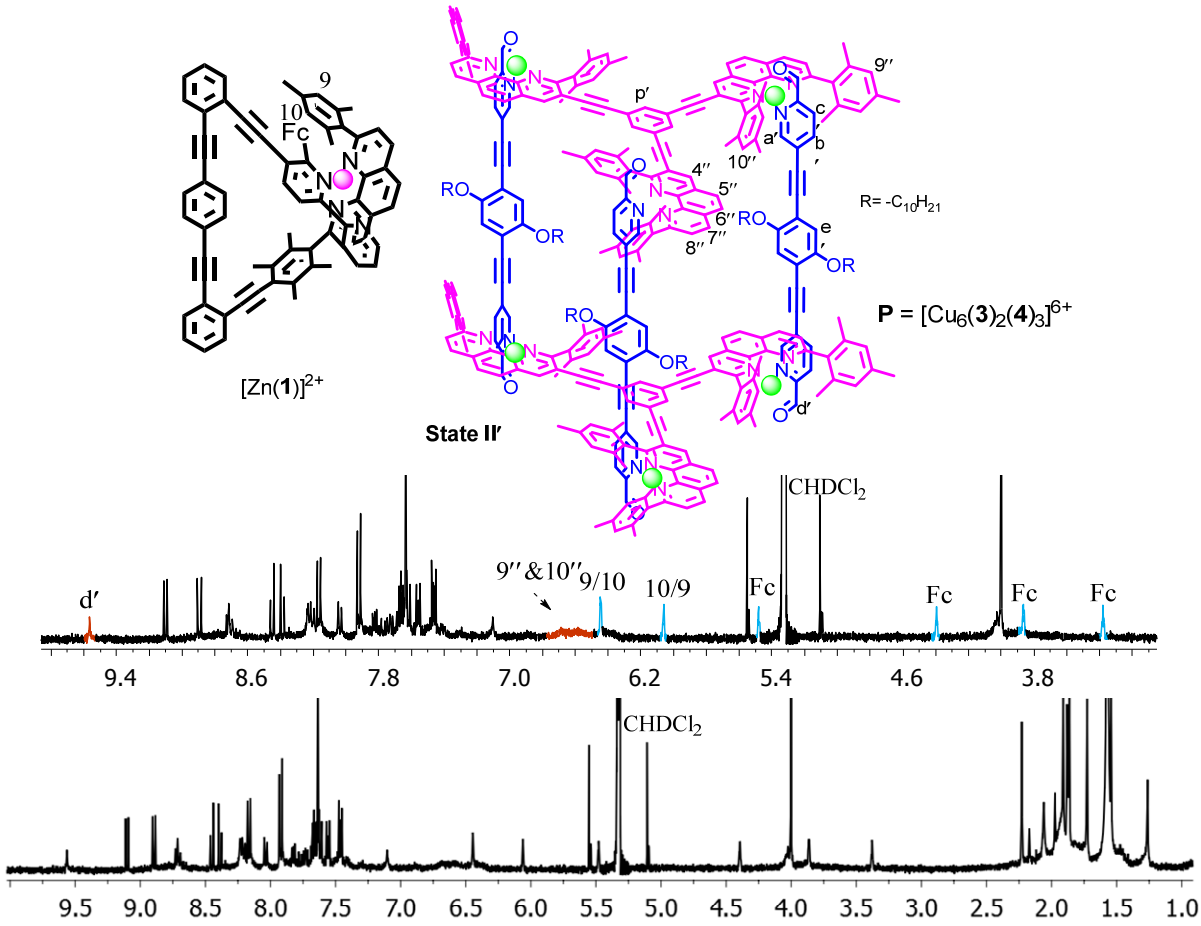

Figure S21: ^{1}H NMR spectra (400 MHz, CD_2Cl_2, 298 K) of State II' = 4 × $[Zn(\mathbf{1})]^{2+}$+ $[Cu_6(\mathbf{3})_2(\mathbf{4})_3]^{6+}$. An expanded part of the aromatic region is shown at the top with characteristic protons assigned.

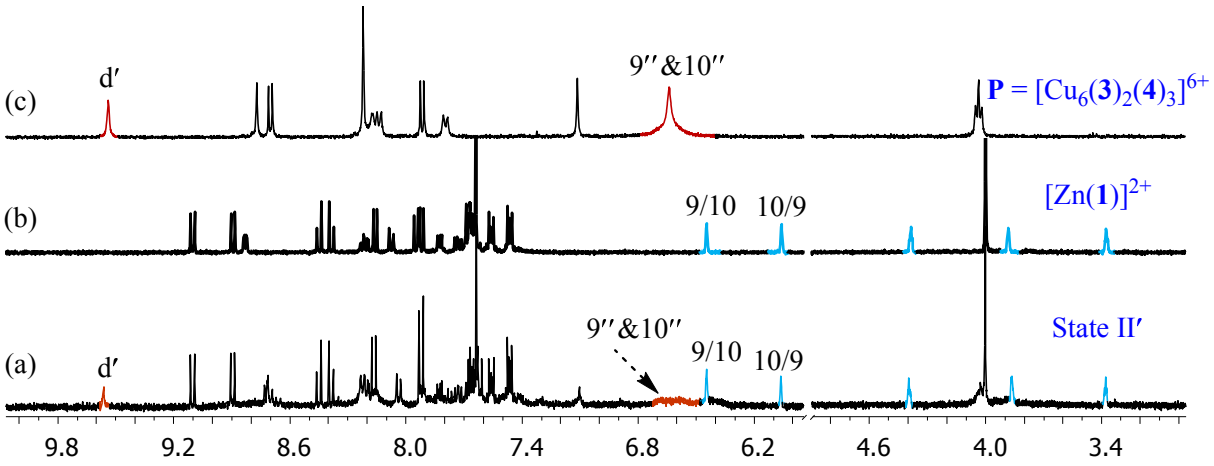

Figure S22: Partial ^{1}H NMR spectra for comparison (400 MHz, CD_2Cl_2, 298 K) of (a) State II′, (b) $[Cu_3(\mathbf{3})_2(\mathbf{4})_3]^{6+}$, (c) $[Zn(\mathbf{1})]^{2+}$.

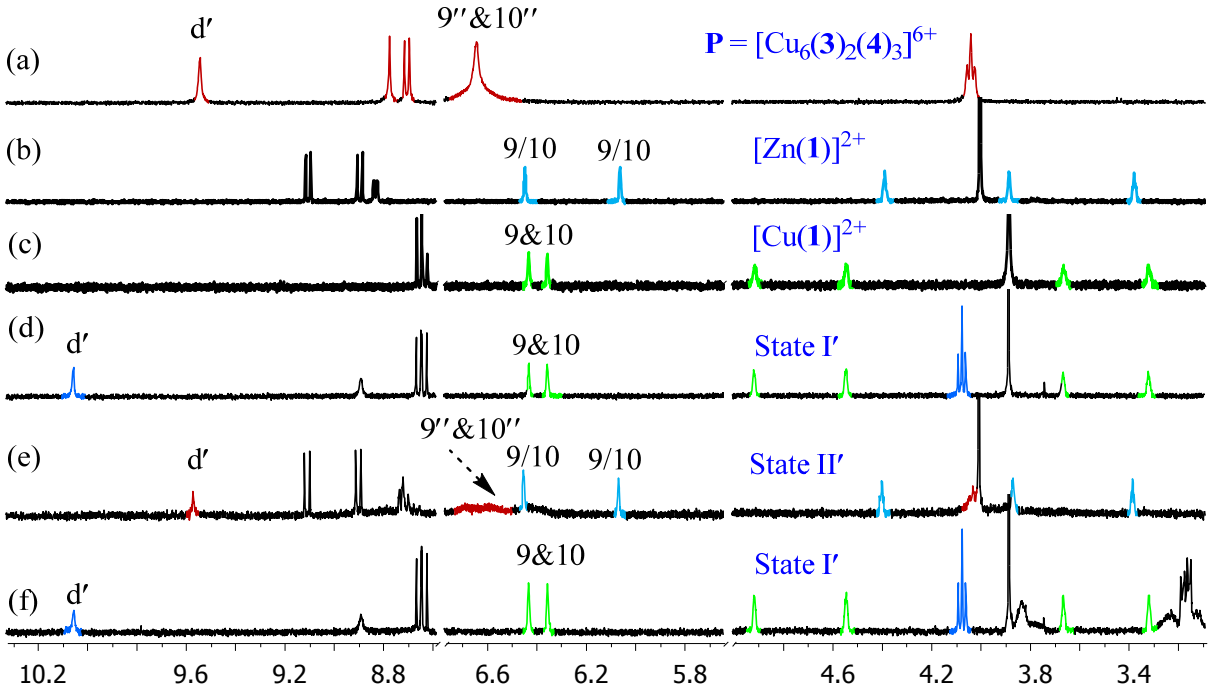

Figure S23: ^{1}H NMR (400 MHz, 298 K, CD_2Cl_2) showing *in-situ* reversible assembly and disassembly of prism **P** by nanoswitch **1**. (a) **P**= $[Cu_6(\mathbf{3})_2(\mathbf{4})_3](PF_6)_6$; (b) $[Zn(\mathbf{1})]^{2+}$; (c) $[Cu(\mathbf{1})]^{+}$; (d) nanoswitch **1**, ligand **3**, **4** and $[Cu(CH_3CN)_4]PF_6$ were mixed in 6:2:3:6 ratio affording state I′; (e) addition of 6 equiv. $Zn(OTf)_2$ to state I′ depicted in spectrum (a) generated state II′, i.e. $[Zn(\mathbf{1})]^{2+}$ + $[Cu_6(\mathbf{3})_2(\mathbf{4})_3]^{6+}$; (f) addition of 4 equiv. of hexacyclen to remove Zn^{2+}, regenerated state I′ along with complex $[Zn(hexacyclen)]^{2+}$.

4 ESI-MS spectra

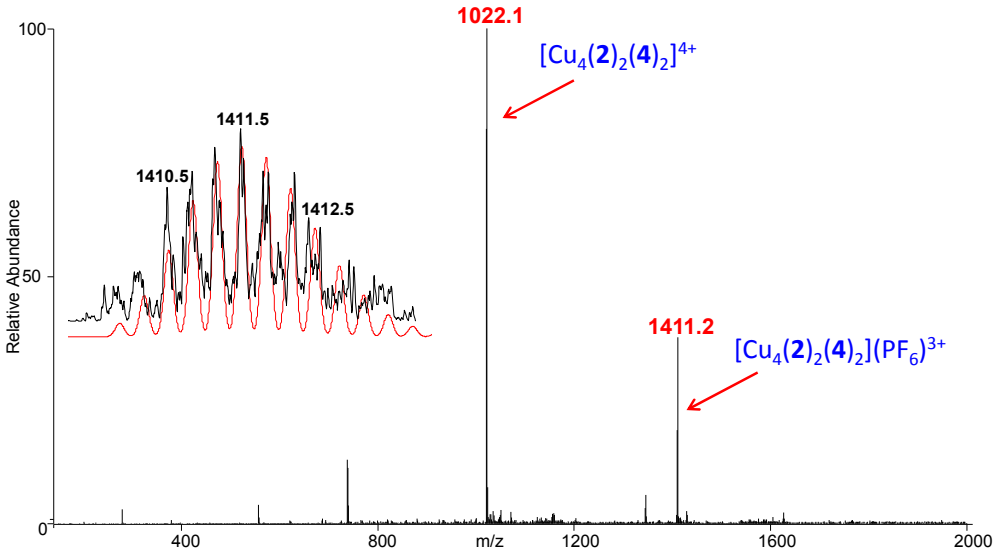

Figure S24: ESI-MS spectrum of 2D rectangle **R** = $[Cu_4(\mathbf{2})_2(\mathbf{4})_2](PF_6)_4$ in CH_2Cl_2 as well as experimental (black lines) and calculated isotopic distributions (red lines) for the peaks associated with $[Cu_4(\mathbf{2})_2(\mathbf{4})_2](PF_6)^{3+}$.

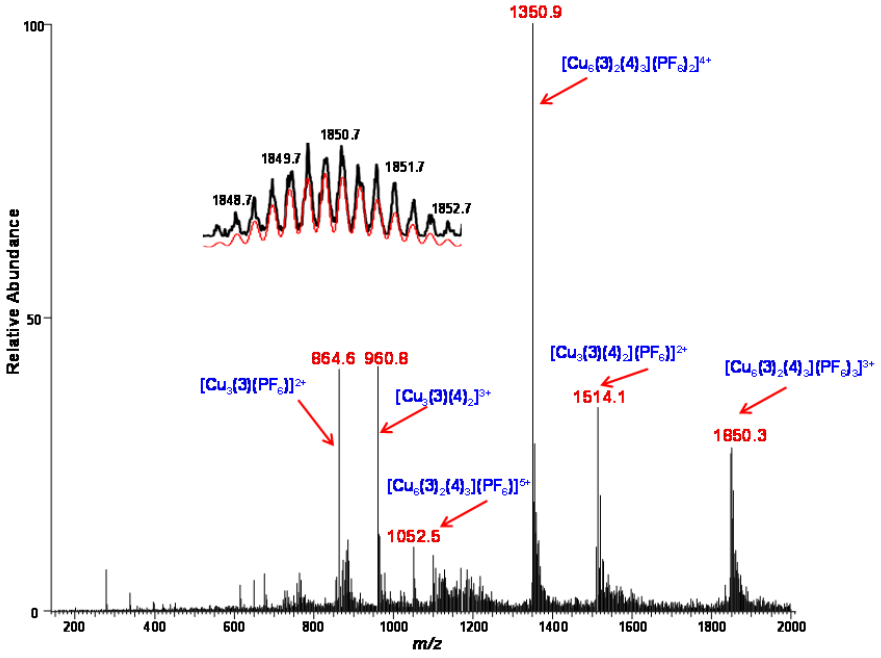

Figure S25: ESI-MS spectrum of prism **P** = $[Cu_6(\mathbf{3})_2(\mathbf{4})_3](PF_6)_6$ in CH_2Cl_2 as well as experimental (black lines) and calculated isotopic distributions (red lines) for the peak associated with $[Cu_6(\mathbf{3})_2(\mathbf{4})_3](PF_6)_3^{3+}$.

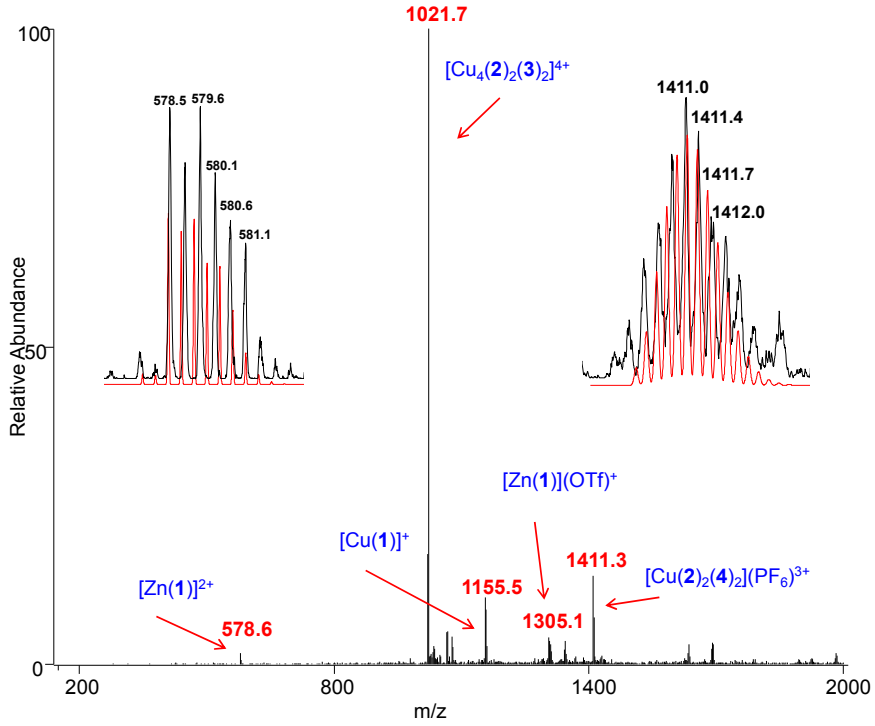

Figure S26: ESI-MS spectrum of State II, i.e. $[Zn(\mathbf{1})]^{2+}$ + Rectangle **R** = $[Cu_4(\mathbf{2})_2(\mathbf{4})_2](PF_6)_4$ in CH_2Cl_2 as well as experimental (black lines) and calculated isotopic distributions (red lines) for the peaks associated with $[Cu_4(\mathbf{2})_2(\mathbf{4})_2](PF_6)^{3+}$ and $[Zn(\mathbf{1})]^{2+}$.

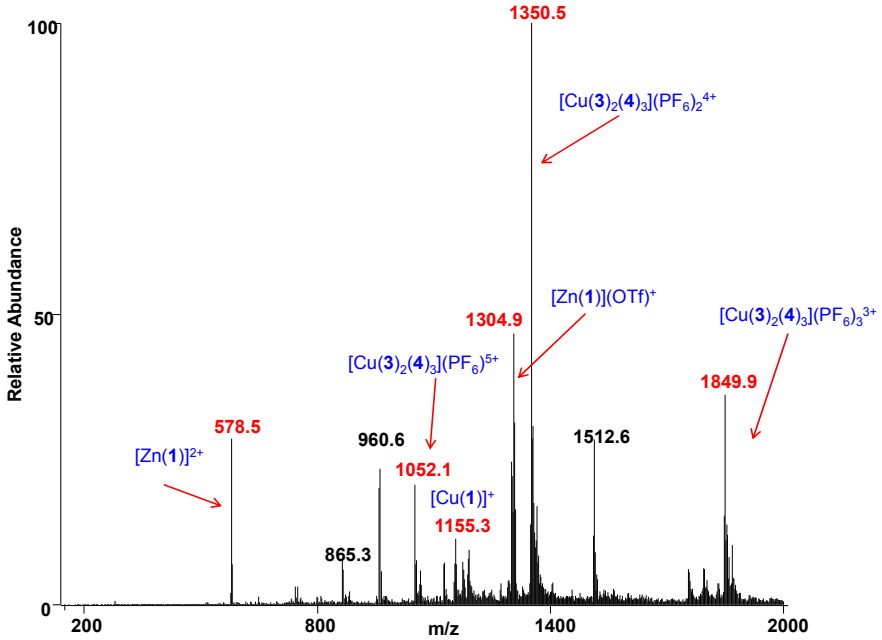

Figure S27: ESI-MS spectrum of State II', i.e., $[Zn(\mathbf{1})]^{2+}$ + Prism **P** = $[Cu_6(\mathbf{3})_2(\mathbf{4})_3](PF_6)_6$ in CH_2Cl_2.

5 UV-vis Data

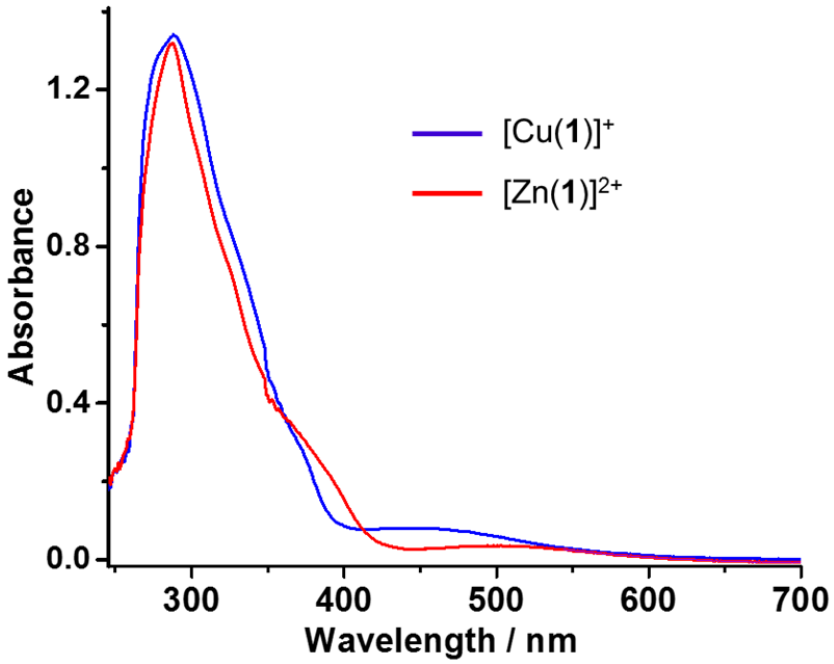

Figure S28. UV-vis spectra of complexes $[Cu(\mathbf{1})]^{+}$ and $[Zn(\mathbf{1})]^{2+}$ in CH_2Cl_2 (10^{-5} M) at 298 K.

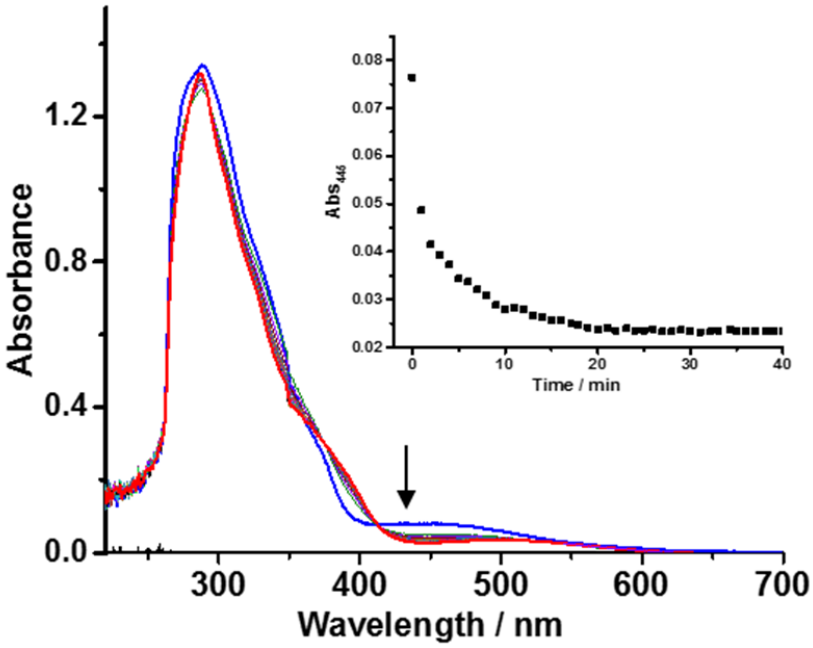

Figure S29. UV-vis spectra taken during the kinetic study of $[Cu(1)]^{+}$ upon addition of $Zn(OTf)_2$ to afford $[Zn(1)]^{2+}$ in CH_2Cl_2 (10^{-5} M) at 298 K.

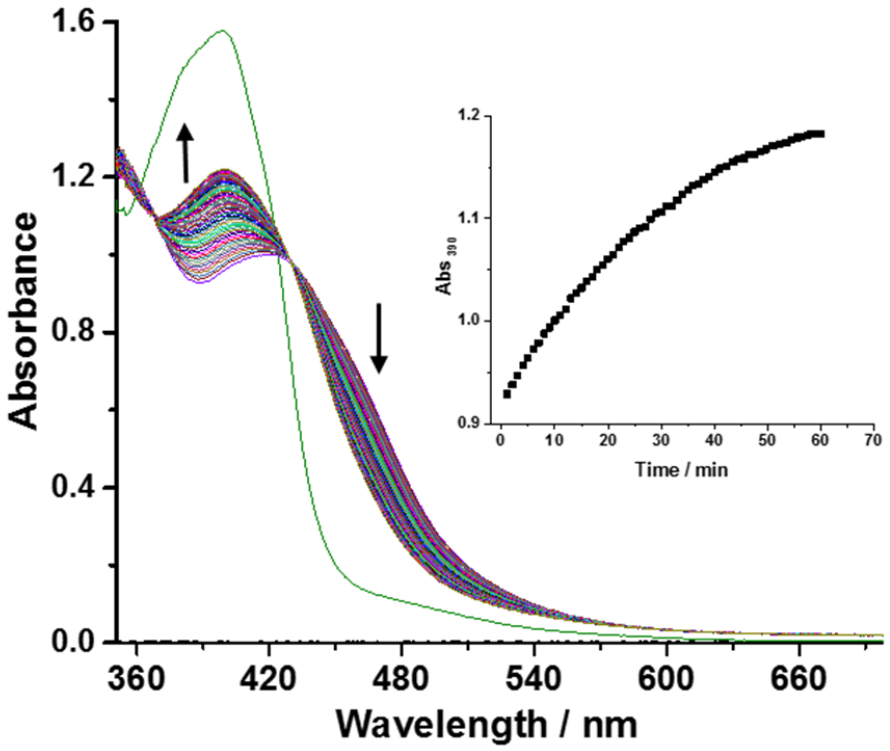

Figure S30. UV-vis spectra taken during the kinetic study (at 1×10^{-5} M) of ($[Cu(\mathbf{1})]^{+}$+**2**+**4**) (= State I) upon addition of $Zn(OTf)_2$ to furnish ($[Zn(\mathbf{1})]^{2+}$ + **R**) in CH_2Cl_2 at 298 K.

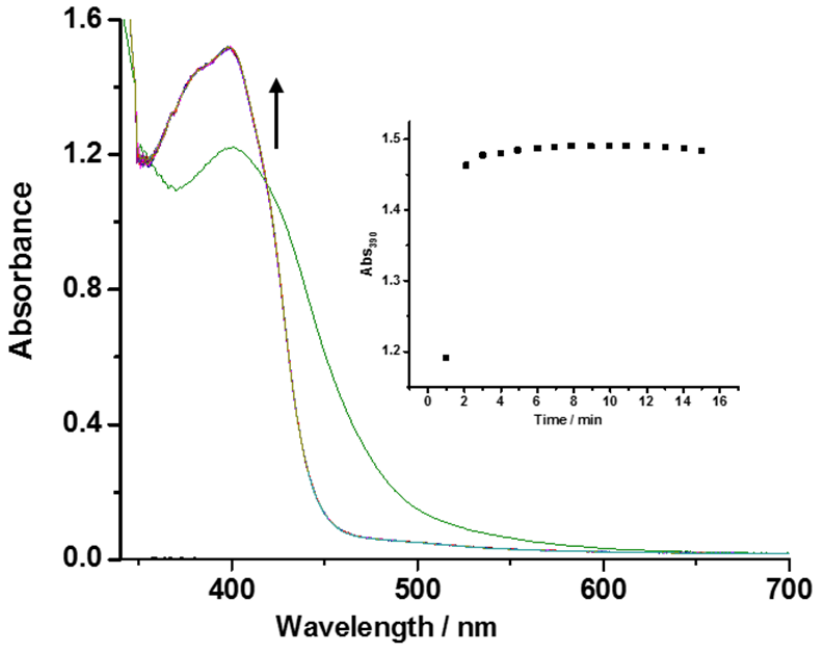

Figure S31. UV-vis spectra taken during the kinetic study of ($[Zn(\mathbf{1})]^{2+}$ + **R**) (=State II) upon addition of hexacyclen to furnish ($[Cu(\mathbf{1})]^{+}$+**2**+**4**) (=State I) in CH_2Cl_2 (at 1×10^{-5} M) at 298 K.

5 DOSY NMR

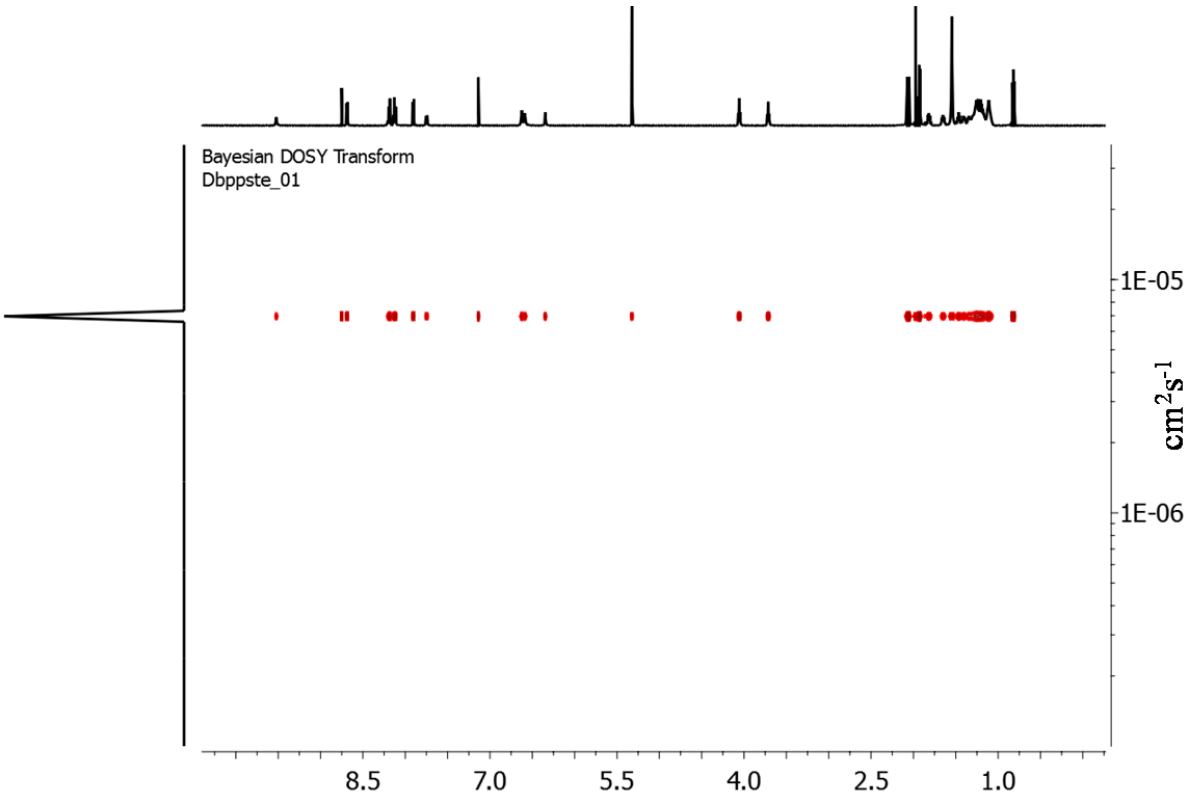

Figure S32: DOSY-NMR spectrum (600 MHz, CD_2Cl_2, 298 K) of rectangle **R** = $[Cu_4(\mathbf{2})_2(\mathbf{4})_2](PF_6)_4$ showing a single diffusion coefficient: $D = 4.6 \times 10^{-10}$ m^2 s^{-1}.

References

1 Schmittel, M.; Pramanik, S.; De, S. *Chem. Commun*. **2012**, *48*, 11730-11732.

2 De, S.; Pramanik, S.; Schmittel, M. *Dalton Trans*. **2014**, *43*, 10977-10982.

3 Wagner, R. W.; Johnson, T. E.; Lindsey, J. S. *J. Am. Chem. Soc.* **1996**, *118*, 11166.

4 Hedbern, F. L.; Rosenberg, H. *Tetrahedron Lett*. **1969**, *10*, 4011.

5 Schmittel, M.; Michel, C.; Wiegrefe, A.; Kalsani, V. *Synthesis* **2001**, *10*, 1561.

6 Singh, R.; Meena J. S.; Wua C-S.; Ko, F-H. *Phys. Chem. Chem. Phys.*, **2015**, *17*, 5227–5235.

7 Goswami, A.; Pramanik, S.; Schmittel, M. *Chem. Commun*. **2018**, *54*, 3955–3958.